
Article:
Tian, Y., Liu, W. orcid.org/0000-0003-2968-2888, Xu, H. et al. (2 more authors) (2022) 2-D DOA estimation of incoherently distributed sources considering gain-phase perturbations in massive MIMO systems. IEEE Transactions on Wireless Communications, 21 (2). pp. 1143-1155. ISSN 1536-1276

https://doi.org/10.1109/twc.2021.3102483

2-D DOA Estimation of Incoherently Distributed Sources Considering Gain-Phase Perturbations in Massive MIMO Systems

Ye Tian, *Member, IEEE*, Wei Liu, *Senior Member, IEEE*, He Xu, Shuai Liu, *Member, IEEE*, and Zhiyan Dong

***Abstract*—In massive multiple-input multiple-output (MIMO) systems, accurate direction-of-arrival (DOA) estimation is important for the base station (BS) to perform effective downlink beamforming. So far, there have been few reports on DOA estimation considering gain-phase perturbations in massive MIMO systems. However, gain-phase perturbations indeed exist in practical applications and cannot be ignored. In this paper, an efficient method for two-dimensional (2-D) DOA estimation of incoherently distributed (ID) sources considering array gain-phase perturbations is proposed for massive MIMO systems. Firstly, a shift invariance structure is established in the subspace framework, and a constrained optimization problem is formulated to estimate the nominal azimuth and elevation DOAs as well as gain-phase perturbations with closed-form expressions, under the assumption that some of the BS antennas are well calibrated; secondly, the corresponding angular spreads are obtained with the aid of the estimated gain-phase perturbations. Theoretical analysis and an approximate Cramér-Rao bound are also provided. An improved estimation performance is achieved by the proposed method as demonstrated by numerical simulations.**

***Index Terms*—2-D DOA estimation, incoherently distributed sources, gain-phase perturbations, massive multiple-input multiple-output (MIMO), partially calibrated.**

I. Introduction

MASSIVE or large-scale multiple-input multiple-output (MIMO) is an enabling technology for the fifth-generation (5G) cellular network, and has received increasing attentions in recent years [1]. A massive MIMO system typically is equipped with hundreds of antennas at each base station (BS), and can provide much higher degrees of freedom (DOFs) to enhance capacity, link reliability and energy efficiency of a wireless communication system given a fixed bandwidth [2]-[4]. According to the realistic transmission environment as well as restricted antenna installation conditions, two-dimensional (2-D) massive MIMO systems have been demonstrated by fitting a large number of antenna elements at the BS [5]. In addition to the advantages mentioned above, massive MIMO can offer other benefits, such as reduced latency, simplified multiple access layer and robustness against jamming signals [6].

The advantages/benefits of the massive MIMO technique cannot be fully exploited without accurate DOA estimation, since accurate DOA knowledge is crucial for the BS to perform effective downlink beamforming of pilot symbols to help estimate the channel gains required for signal detection [7]. In addition, the performance of DOA estimation in a wireless communication system also characterizes the achievable rates and the design of an optimal power allocation scheme [8]. As the massive MIMO system is more likely to be implemented in two dimensions in practice [5], some 2-D DOA estimation algorithms for massive MIMO systems have been investigated in recent years, which can be roughly divided into two categories. The first category is based on the point source model, where the basic assumption is that the energy of each source is concentrated at discrete directions or each scattering cluster generates a single propagation path between BS and mobile station. Examples in this category include the tensor-MODE based algorithm [9], the ESPRIT or unitary ESPRIT algorithms [10]-[15], the root-MUSIC algorithm [16] and the time-frequency MUSIC algorithm [17].

The second category is built on a distributed source model, which assumes that one scattering cluster corresponds to multiple propagation paths. This category can be further classified into two subcategories, i.e., 2-D DOA estimation of coherently distributed (CD) sources and incoherently distributed (ID) sources. Compared with the point source model, the distributed source model is more appropriate for cellular wireless communication systems due to the effect of multi-path propagation [18]. The difference between CD sources and ID sources lies in their different channel models. CD sources correspond to slowly time-varying channels, whereas ID sources correspond to rapidly time-varying channels. For DOA estimation of CD sources, both subspace based and sparse reconstruction based algorithms have been proposed by extending the approaches based on the point source model [19]-[23]. Although some of the above algorithms are designed for 1-D DOA estimation of CD sources, they can be easily extended to the 2-D case. However, for ID sources, it is rather complicated since the signal components span the whole observation space. Nevertheless, several 2-D localization algo-

Manuscript received October 10, 2020; revised June 12, 2021; accepted August 1, 2021. This work was supported in part by the National Natural Science Foundation of China under Grants 61601398, 62001256, and in part by the Project of Science and Technology Commission of Shanghai Municipality under Grant 19511132000. (*Corresponding Author: Wei Liu.*)

Y. Tian and H. Xu are with the Faculty of Information Science and Engineering, Ningbo University, Ningbo 315211, China (e-mail: tianfield@126.com; xuhebest@sina.com).

W. Liu is with the Department of Electronic and Electrical Engineering, University of Sheffield, Sheffield S1 3JD, U.K. (e-mail: w.liu@sheffield.ac.uk).

S. Liu is with the School of Information Science and Engineering, Yanshan University, Qinhuangdao 066004, China. (e-mail: liushuai@ysu.edu.cn).

Z. Dong is with the Academy for Engineering and Technology, Fudan University, Shanghai 200433, China, and also with Jihua Lab, Western Road of Nanping, Nanhai Distinct, Foshan 528200, China (e-mail: dongzhiyan@fudan.edu.cn).

rithms for ID sources were also introduced from the subspace theory perspective [24]-[29]. The algorithms presented in [24]-[26] can provide good estimation performance, by employing multi-dimensional optimization or search. However, due to their high computational complexity, these algorithms are not suitable for practical real-time massive MIMO implementations [28], [30]. To reduce computational complexity, an ESPRIT-based approach was investigated [27], which can lead to closed-form solutions without spectral search. Based on [27], low-complexity beamspace-based algorithms for uniform rectangular arrays (URAs) and uniform circular arrays (UCAs) were proposed in [28] and [29], respectively.

All the methods mentioned above assume that the steering vector of the antenna array is known. However, there are unknown array perturbations (such as gain-phase perturbations, mutual coupling and array geometry errors) in practice, and they can significantly degrade the performance of DOA estimation algorithms [31]-[33]. Although there have been many algorithms for DOA estimation in the presence of array perturbations [34]-[37], most of them are based on the point source model. Moreover, some of these algorithms have a very high computational complexity and cannot be used for a practical massive MIMO system. Recently, an algorithm based on the ESPRIT technique for 1-D DOA estimation of CD sources with unknown mutual coupling was proposed [38], but it cannot be extended to ID sources and 2-D DOA estimation since it relies on a special structure of array covariance matrix. There is a clear gap in literature for 2-D DOA estimation of ID sources with array perturbations.

In this paper, the problem of 2-D DOA estimation for ID sources with array perturbations in massive MIMO systems is addressed, where the array gain-phase perturbations mainly caused by imperfect amplifier and phase synchronization (or more specifically, caused by phase noise of the local oscillator [39], [40], the capacitor mismatch [41] and errors in down-sampling due to clock drifting by the local oscillator [42]) are considered, and the other array perturbations (whose influence and calibration will be a topic of our further research) are assumed to have been compensated in some way. Given the fact that it is typically difficult to calibrate the whole large-scale array, while a relatively small part of such an array can be easily calibrated [43], [44], the partly calibrated uniform rectangular array (URA) is considered here. Based on the ESPRIT and constrained least squares techniques, the 2-D nominal DOAs, their related angular spreads and the gain-phase perturbations can be jointly estimated in closed-form expressions, which is a computationally efficient way and suitable for practical real-time massive MIMO implementations. Notice that the robust versions of ESPRIT against array gain-phase perturbations have been proposed in the literature [45], [46]. However, they are all established on the point source model and uniform/nonuniform linear arrays, and cannot deal with our considered scenario. The main contributions of this paper are listed as follows.

1) To the best of our knowledge, it is the first time to address the problem of 2-D DOA estimation for ID sources with array perturbations. An efficient scheme is proposed for 2-D DOA, angular spread estimation and gain-phase perturbations calibration, under the condition that part of array antennas are well calibrated.
2) The influence of gain-phase perturbations on the performance of the ESPRIT-based approach is analyzed and a condition on the minimal number of calibrated antennas required to calibrate the whole array is derived.
3) An approximate Cramér-Rao bound (CRB) for 2-D DOA estimation of ID sources with gain-phase perturbations is derived, which matches better with the adopted approximate signal model, compared with the existing CRB.

The rest of this paper is organized as follows. The problem is formulated in Section II and the joint estimation algorithm for 2-D DOA, angular spreads and gain-phase perturbations is presented in Section III. In Section IV, performance analysis of the proposed method is provided including the influence of gain-phase perturbations, the minimal number of required calibrated antennas, and the approximate CRB. Numerical simulations are provided in Section V and conclusions are drawn in Section VI.

Notations: Throughout the paper, we use upper-case (lower-case) bold letters to represent matrices (vectors). $\mathbf{I}_M$ denotes the $M\times M$ identity matrix, $\mathbf{1}_P$ denotes the all-one $P\times 1$ vector, $\mathbf{e}_m$ stands for a vector whose mth element equals one and zeros elsewhere, and $\mathbf{0}_{P\times Q}$ stands for the $P\times Q$ zero matrix. $(\cdot)^*, (\cdot)^T, (\cdot)^H$ and $(\cdot)^{-1}$ represent the conjugate, transpose, conjugate transpose and inversion operations, respectively. The symbols $\odot$ and $\otimes$ stand for the Schur-Hadamard product and the Kronecker product, respectively. $\mathbb{E}\{\cdot\}$ is the statistical expectation, $\mathrm{Re}\{\cdot\}$ and $\mathrm{Im}\{\cdot\}$ the real part and imaginary part of a complex value, respectively, $\delta(\cdot)$ the Kronecker delta function, $\mathrm{Tr}(\cdot)$ and $\|\cdot\|_F$ the trace and the Frobenius norm of a matrix, respectively, $\mathrm{diag}\{z_1, z_2\}$ a diagonal matrix with its diagonal elements z_1 and z_2, $\mathrm{blkdiag}(\cdot)$ the block-diagonalization operation, $\angle[\cdot]$ the phase of a complex number. $[\cdot]_{m,n}$ is the (m,n)th element of a matrix, and $[\cdot]_m$ the mth element of a vector.

II. Problem Formulation

A. Ideal URA Model

Consider that K uncorrelated narrowband ID sources transmitted by user equipments (UEs) impinge on an M-element ideal URA of the BS in a massive MIMO system, as illustrated in Fig. 1, where $M = M_xM_y$ with M_x and M_y being the number of antennas in the x-direction and y-direction, respectively. The array output observed at time instant t, $t = 1, 2, \ldots, N$, can be expressed as [27], [28]

$$\mathbf{x}(t) = \sum_{k=1}^{K} s_k(t) \sum_{l=1}^{L_k} \gamma_{k,l}(t)\mathbf{a}(\theta_{k,l}(t), \phi_{k,l}(t)) + \mathbf{n}(t), \quad (1)$$

where $s_k(t)$ and $\mathbf{n}(t)$ are the signal transmitted by the kth UE and the $M\times 1$ additive noise vector, respectively, $\gamma_{k,l}(t)$ is the complex-valued path gain, and L_k is the number of multipaths of the kth UE. $0 \le \theta_{k,l}(t) = \theta_k + \tilde{\theta}_{k,l}(t) < \pi$ and $0 \le \phi_{k,l}(t) = \phi_k + \tilde{\phi}_{k,l}(t) < \pi/2$, where θ_k and ϕ_k are the nominal azimuth and elevation DOAs for the kth

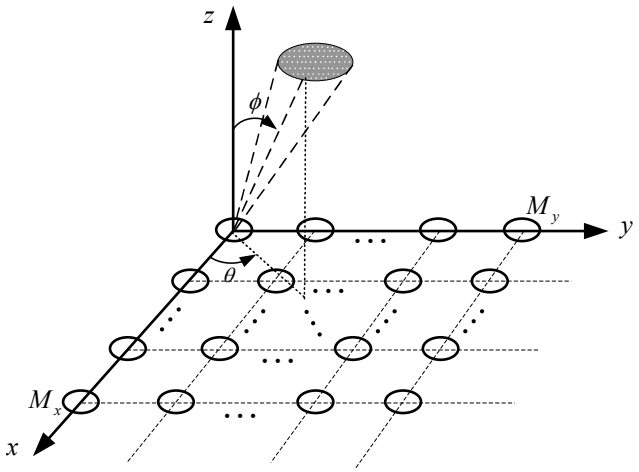

Fig. 1. URA geometry for massive MIMO system.

signal, while $\tilde{\theta}_{k,l}(t)$ and $\tilde{\phi}_{k,l}(t)$ are the corresponding random angular deviations with zero mean and standard deviations σ_{θ_k} and σ_{ϕ_k}. $\mathbf{a}(\theta_{k,l}(t), \phi_{k,l}(t))$ denotes the steering vector of the kth source signal.

Taking the origin of the axes as the phase reference point and further exploiting the first order Taylor series expansion of $\mathbf{a}(\theta_{k,l}(t), \phi_{k,l}(t))$ under the conditions that σ_{θ_k} and σ_{ϕ_k} are sufficiently small, $\mathbf{a}(\theta_{k,l}(t), \phi_{k,l}(t))$ can be approximately expressed as [27], [28]

$$\begin{aligned}\mathbf{a}(\theta_{k,l}(t), \phi_{k,l}(t)) \approx \mathbf{a}(\theta_k, \phi_k) + \frac{\partial \mathbf{a}(\theta_k, \phi_k)}{\partial \theta_k}\tilde{\theta}_{k,l}(t) \\ + \frac{\partial \mathbf{a}(\theta_k, \phi_k)}{\partial \phi_k}\tilde{\phi}_{k,l}(t),\end{aligned} \tag{2}$$

where the mth element of $\mathbf{a}(\theta_k, \phi_k)$ is given by

$$\begin{aligned}[\mathbf{a}(\theta_k, \phi_k)]_m = \exp(ju\sin\phi_k[(m_x-1)\cos\theta_k \\ + (m_y-1)\sin\theta_k]), m = (m_y-1)M_x + m_x, \\ m_x = 1, 2, \ldots, M_x, m_y = 1, 2, \ldots, M_y,\end{aligned} \tag{3}$$

with $u = 2\pi d/\lambda$, d being the adjacent sensor distance along the x and y axes of the array, and λ being the wavelength of the carrier.

Consequently, the array output $\mathbf{x}(t)$ in (1) can be written as

$$\mathbf{x}(t) \approx \mathbf{A}(\theta, \phi)\bar{\mathbf{s}}(t) + \mathbf{n}(t), \tag{4}$$

where

$$\begin{aligned}\mathbf{A}(\theta, \phi) = \Big[\mathbf{a}(\theta_1, \phi_1), \mathbf{a}(\theta_2, \phi_2), \ldots, \mathbf{a}(\theta_K, \phi_K), \\ \frac{\partial \mathbf{a}(\theta_1, \phi_1)}{\partial \theta_1}, \frac{\partial \mathbf{a}(\theta_2, \phi_2)}{\partial \theta_2}, \ldots, \frac{\partial \mathbf{a}(\theta_K, \phi_K)}{\partial \theta_K}, \\ \frac{\partial \mathbf{a}(\theta_1, \phi_1)}{\partial \phi_1}, \frac{\partial \mathbf{a}(\theta_2, \phi_2)}{\partial \phi_2}, \ldots, \frac{\partial \mathbf{a}(\theta_K, \phi_K)}{\partial \phi_K}\Big],\end{aligned} \tag{5}$$

$$\begin{aligned}\bar{\mathbf{s}}(t) = [\bar{s}_{1,1}(t), \bar{s}_{2,1}(t), \ldots, \bar{s}_{K,1}(t), \bar{s}_{1,2}(t), \bar{s}_{2,2}(t), \ldots, \\ \bar{s}_{K,2}(t), \bar{s}_{1,3}(t), \bar{s}_{2,3}(t), \ldots, \bar{s}_{K,3}(t)]^T,\end{aligned} \tag{6}$$

$$\bar{s}_{k,1}(t) = s_k(t)\sum_{l=1}^{L_k}\gamma_{k,l}(t), \tag{7}$$

$$\bar{s}_{k,2}(t) = s_k(t)\sum_{l=1}^{L_k}\gamma_{k,l}(t)\tilde{\theta}_{k,l}(t), \tag{8}$$

$$\bar{s}_{k,3}(t) = s_k(t)\sum_{l=1}^{L_k}\gamma_{k,l}(t)\tilde{\phi}_{k,l}(t). \tag{9}$$

B. Partly Calibrated URA Model

Now consider the case that only part of the URA is well calibrated. Without loss of generality, assume that the first P rows and Q columns of antennas of the array are calibrated, whereas the remaining $M - PQ$ antennas are uncalibrated with perturbations modeled as unknown, direction-independent gains and phases. Taking these unknown gain-phase perturbations into account, the array output can be given by

$$\begin{aligned}\mathbf{y}(t) &= \mathbf{\Phi}(\mu)\sum_{k=1}^{K}s_k(t)\sum_{l=1}^{L_k}\gamma_{k,l}(t)\mathbf{a}(\theta_{k,l}(t), \phi_{k,l}(t)) + \mathbf{n}(t) \\ &\approx \mathbf{\Phi}(\mu)\mathbf{A}(\theta, \phi)\bar{\mathbf{s}}(t) + \mathbf{n}(t),\end{aligned} \tag{10}$$

where $\mathbf{\Phi}(\mu)$ denotes the gain-phase perturbation matrix, and is expressed as

$$\mathbf{\Phi}(\mu) = \mathrm{diag}\{[\mathbf{c}, \mu_{QM_x+1}, \ldots, \mu_{M_xM_y}]\}, \tag{11}$$

where

$$\mathbf{c} = \underbrace{[\mathbf{1}_P^T, \mu_{P+1}, \ldots, \mu_{M_x}, \ldots, \mathbf{1}_P^T, \mu_{(Q-1)M_x+P+1}, \ldots, \mu_{QM_x}]}_{1\times QM_x} \tag{12}$$

is a vector composed of the gain-phase perturbations of the first M_xQ (M_x rows $\times$ Q columns) antennas of the array, $\mu_m = \rho_m e^{j\psi_m}$ with ρ_m and ψ_m representing the gain perturbation and phase perturbation of the antenna located at the m_1th row and m_2th column of the URA, $m = (m_2-1)M_x + m_1$, $m_1 \in [1, M_x]$, $m_2 \in [1, M_y]$.

In addition, we also make the following assumptions:

- The signals $s_k(t)$, $k = 1, \ldots, K$, are zero-mean, complex-valued and temporally independent and identically distributed (i.i.d.) random variables with covariance $\sigma_{s_k}^2$. The noise $\mathbf{n}(t)$ is stationary, zero-mean and spatially white Gaussian with covariance matrix $\sigma_n^2\mathbf{I}_M$.
- The angular deviations $\tilde{\theta}_{k,l}(t)$, $\tilde{\phi}_{k,l}(t)$ and the path gains $\gamma_{k,l}(t)$ are temporally i.i.d. Gaussian random variables with covariances given by [27], [28]

$$\mathbb{E}\{\tilde{\theta}_{k,l}(t)\tilde{\theta}_{\bar{k},\bar{l}}(\bar{t})\} = \sigma_\theta^2\delta(k-\bar{k})\delta(l-\bar{l})\delta(t-\bar{t}), \tag{13}$$

$$\mathbb{E}\{\tilde{\phi}_{k,l}(t)\tilde{\phi}_{\bar{k},\bar{l}}(\bar{t})\} = \sigma_\phi^2\delta(k-\bar{k})\delta(l-\bar{l})\delta(t-\bar{t}), \tag{14}$$

$$\mathbb{E}\{\gamma_{k,l}(t)\gamma_{\bar{k},\bar{l}}(\bar{t})\} = \frac{\sigma_\gamma^2}{L_k}\delta(k-\bar{k})\delta(l-\bar{l})\delta(t-\bar{t}). \tag{15}$$

- The transmitted signals, additive noise, angular deviations and the path gains are mutually uncorrelated.
- The number of UEs K is known a priori or pre-estimated via methods such as those based on the robust LS-MDL criterion [38], [47]. The number of antennas M is much

larger than K, and the number of multipaths L_k is large for any $k \in [1, K]$.
- Part of the array is well calibrated, and the number of calibrated antennas satisfies $P, Q \geq 2$.
- A small angle scattering environment is considered, i.e., the angular spreads σ_{θ_k} and σ_{ϕ_k} $(k = 1, \ldots, K)$ are sufficiently small.

III. Proposed Method

A. 2-D Estimation of Nominal DOAs

According to (10) and the above assumptions, we can obtain the covariance matrix of the received signal $\mathbf{y}(t)$, given by

$$\begin{aligned}\mathbf{R}_y &= \mathbb{E}\left\{\mathbf{y}\left(t\right)\mathbf{y}^H\left(t\right)\right\} \\ &\approx \mathbf{\Phi}(\mu)\mathbf{A}\left(\theta,\phi\right)\mathbf{S}\mathbf{A}^H\left(\theta,\phi\right)\mathbf{\Phi}^H(\mu) + \sigma_n^2\mathbf{I}_M, \end{aligned} \tag{16}$$

where $\mathbf{S} = \mathbb{E}\left\{\bar{\mathbf{s}}\left(t\right)\bar{\mathbf{s}}^H\left(t\right)\right\}$ is a $3K \times 3K$ diagonal matrix with $[\mathbf{S}]_{k,k} = \sigma_k^2\sigma_\gamma^2$, $[\mathbf{S}]_{k+K,k+K} = [\mathbf{S}]_{k,k}\sigma_{\theta_k}^2$, and $[\mathbf{S}]_{k+2K,k+2K} = [\mathbf{S}]_{k,k}\sigma_{\phi_k}^2$, $k \in [1, K]$.

The eigenvalue decomposition (EVD) of $\mathbf{R}_y$ is approximated by

$$\begin{aligned}\mathbf{R}_y &\approx [\mathbf{E}_s, \mathbf{E}_n]\begin{bmatrix}\mathbf{\Lambda}_s & \mathbf{0}_{3K\times(M-3K)} \\ \mathbf{0}_{(M-3K)\times 3K} & \mathbf{\Lambda}_n\end{bmatrix}[\mathbf{E}_s, \mathbf{E}_n]^H \\ &= \mathbf{E}_s\mathbf{\Lambda}_s\mathbf{E}_s^H + \mathbf{E}_n\mathbf{\Lambda}_n\mathbf{E}_n^H, \end{aligned} \tag{17}$$

where $\mathbf{E}_s$ and $\mathbf{E}_n$ are the $M \times 3K$-dimensional signal subspace matrix and the $M \times (M-3K)$-dimensional noise subspace matrix, respectively. $\mathbf{\Lambda}_s$ and $\mathbf{\Lambda}_n$ denote the diagonal matrices comprising the $3K$ largest eigenvalues and the remaining $M-3K$ eigenvalues, respectively. In practice, $\mathbf{R}_y$ is replaced by its finite-sample estimation, i.e.,

$$\mathbf{R}_y \approx \hat{\mathbf{R}}_y = N^{-1}\sum_{t=1}^{N}\mathbf{y}\left(t\right)\mathbf{y}^H\left(t\right) \approx \hat{\mathbf{E}}_S\hat{\mathbf{\Lambda}}_S\hat{\mathbf{E}}_S^H + \hat{\mathbf{E}}_N\hat{\mathbf{\Lambda}}_N\hat{\mathbf{E}}_N^H. \tag{18}$$

Next, we show how to jointly estimate 2-D DOAs, their corresponding angular spreads as well as gain-phase perturbations utilizing $\hat{\mathbf{R}}_y$.

Instead of dividing the received array into three subarrays as in [27], we divide the whole URA into four subarrays as depicted in Fig. 2, which can provide more DOFs. The output of each subarray can be expressed as

$$\mathbf{y}_\tau\left(t\right) = \mathbf{J}_\tau\mathbf{y}\left(t\right) \approx \mathbf{\Phi}_\tau\left(\mu\right)\mathbf{A}_\tau\left(\theta,\phi\right)\bar{\mathbf{s}}\left(t\right) + \mathbf{n}_\tau\left(t\right), \tag{19}$$

where $\mathbf{\Phi}_\tau\left(\mu\right)$ and $\mathbf{A}_\tau\left(\theta,\phi\right)$ denote the gain-phase perturbation matrix and the nominal steering matrix of the τth subarray, respectively, $\tau = 1, \ldots, 4$. $\mathbf{J}_\tau$ is given by

$$\begin{aligned}\mathbf{J}_1 &= \left[\mathbf{I}_{M-M_x}\ \ \mathbf{0}_{(M-M_x)\times M_x}\right], \\ \mathbf{J}_2 &= \left[\mathbf{0}_{(M-M_x)\times M_x}\ \ \mathbf{I}_{M-M_x}\right], \\ \mathbf{J}_3 &= \mathbf{I}_{M_y} \otimes \left[\mathbf{I}_{M_x-1}\ \ \mathbf{0}_{(M_x-1)\times 1}\right], \\ \mathbf{J}_4 &= \mathbf{I}_{M_y} \otimes \left[\mathbf{0}_{(M_x-1)\times 1}\ \ \mathbf{I}_{M_x-1}\right]. \end{aligned}$$

According to locations of these four subarrays, the following relationships hold

$$\mathbf{A}_2\left(\theta,\phi\right) = \mathbf{A}_1\left(\theta,\phi\right)\mathbf{\Omega}_{2,1}, \tag{20}$$

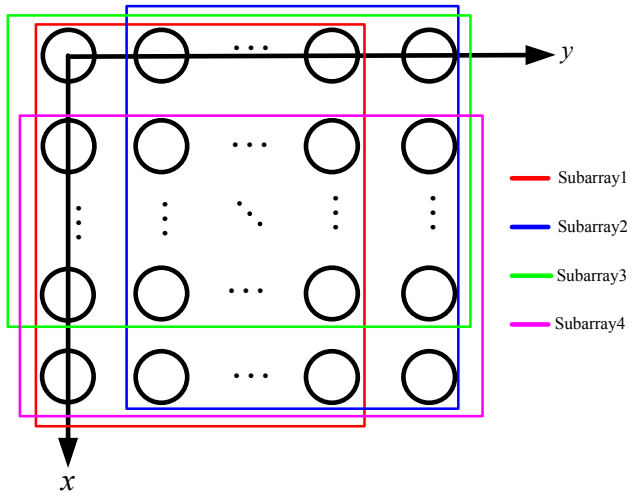

Fig. 2. The four considered subarrays of the URA.

$$\mathbf{A}_4\left(\theta,\phi\right) = \mathbf{A}_3\left(\theta,\phi\right)\mathbf{\Omega}_{4,3}, \tag{21}$$

where

$$\mathbf{\Omega}_{2,1} = \begin{bmatrix}\mathbf{\Pi}_{2,1} & \mathbf{\Pi}_{2,2} & \mathbf{\Pi}_{2,3} \\ \mathbf{0}_{K\times K} & \mathbf{\Pi}_{2,1} & \mathbf{0}_{K\times K} \\ \mathbf{0}_{K\times K} & \mathbf{0}_{K\times K} & \mathbf{\Pi}_{2,1}\end{bmatrix} \in \mathbb{C}^{3K\times 3K}, \tag{22}$$

$$\mathbf{\Omega}_{4,3} = \begin{bmatrix}\mathbf{\Xi}_{4,3} & \mathbf{\Xi}_{4,4} & \mathbf{\Xi}_{4,5} \\ \mathbf{0}_{K\times K} & \mathbf{\Xi}_{4,3} & \mathbf{0}_{K\times K} \\ \mathbf{0}_{K\times K} & \mathbf{0}_{K\times K} & \mathbf{\Xi}_{4,3}\end{bmatrix} \in \mathbb{C}^{3K\times 3K}, \tag{23}$$

$$\mathbf{\Pi}_{2,1} = \mathrm{diag}\left(H_2\left(\theta_1,\phi_1\right),\ldots,H_2\left(\theta_K,\phi_K\right)\right), \tag{24}$$

$$\mathbf{\Xi}_{4,3} = \mathrm{diag}\left(H_4\left(\theta_1,\phi_1\right),\ldots,H_4\left(\theta_K,\phi_K\right)\right), \tag{25}$$

$$\mathbf{\Pi}_{2,2} = \mathrm{diag}\left(\frac{\partial H_2\left(\theta_1,\phi_1\right)}{\partial\theta_1},\ldots,\frac{\partial H_2\left(\theta_K,\phi_K\right)}{\partial\theta_K}\right), \tag{26}$$

$$\mathbf{\Xi}_{4,4} = \mathrm{diag}\left(\frac{\partial H_4\left(\theta_1,\phi_1\right)}{\partial\theta_1},\ldots,\frac{\partial H_4\left(\theta_K,\phi_K\right)}{\partial\theta_K}\right), \tag{27}$$

$$\mathbf{\Pi}_{2,3} = \mathrm{diag}\left(\frac{\partial H_2\left(\theta_1,\phi_1\right)}{\partial\phi_1},\ldots,\frac{\partial H_2\left(\theta_K,\phi_K\right)}{\partial\phi_K}\right), \tag{28}$$

$$\mathbf{\Xi}_{4,5} = \mathrm{diag}\left(\frac{\partial H_4\left(\theta_1,\phi_1\right)}{\partial\phi_1},\ldots,\frac{\partial H_4\left(\theta_K,\phi_K\right)}{\partial\phi_K}\right), \tag{29}$$

with $H_2\left(\theta_1,\phi_1\right) = \exp\left(ju\sin\phi_k\sin\theta_k\right)$ and $H_4\left(\theta_1,\phi_1\right) = \exp\left(ju\sin\phi_k\cos\theta_k\right)$.

It is well known that the signal subspace $\mathbf{E}_s$ spans the same space as the array steering matrix; then, we have

$$\mathbf{E}_s = \mathbf{\Phi}(\mu)\mathbf{A}\left(\theta,\phi\right)\mathbf{T}, \tag{30}$$

where $\mathbf{T}$ is an $3K \times 3K$ nonsingular matrix. Subsequently, (30) directly yields

$$\mathbf{E}_{s1} = \mathbf{J}_1\mathbf{E}_s = \mathbf{\Phi}_1(\mu)\mathbf{A}_1\left(\theta,\phi\right)\mathbf{T}, \tag{31}$$

$$\mathbf{E}_{s2} = \mathbf{J}_2\mathbf{E}_s = \mathbf{\Phi}_2(\mu)\mathbf{A}_2\left(\theta,\phi\right)\mathbf{T}, \tag{32}$$

$$\mathbf{E}_{s3} = \mathbf{J}_3\mathbf{E}_s = \mathbf{\Phi}_3(\mu)\mathbf{A}_3\left(\theta,\phi\right)\mathbf{T}, \tag{33}$$

$$\mathbf{E}_{s4} = \mathbf{J}_4\mathbf{E}_s = \mathbf{\Phi}_4(\mu)\mathbf{A}_4\left(\theta,\phi\right)\mathbf{T}. \tag{34}$$

Substituting (20), (21) into (32) and (34), respectively, we have

$$\mathbf{\Phi}_{1,2}(\mu)\mathbf{E}_{s2} = \mathbf{E}_{s1}\mathbf{\Psi}_{2,1}, \tag{35}$$

$$\mathbf{\Phi}_{3,4}(\mu)\mathbf{E}_{s4} = \mathbf{E}_{s3}\mathbf{\Psi}_{4,3}, \tag{36}$$

where

$$\mathbf{\Psi}_{2,1} = \mathbf{T}^{-1}\mathbf{\Omega}_{2,1}\mathbf{T}, \mathbf{\Psi}_{4,3} = \mathbf{T}^{-1}\mathbf{\Omega}_{4,3}\mathbf{T}, \tag{37}$$

$$\mathbf{\Phi}_{1,2}(\mu) = \mathbf{\Phi}_1(\mu)/\mathbf{\Phi}_2(\mu) = \mathrm{diag}(\bar{\mathbf{c}}), \tag{38}$$

$$\mathbf{\Phi}_{3,4}(\mu) = \mathbf{\Phi}_3(\mu)/\mathbf{\Phi}_4(\mu) = \mathrm{diag}(\tilde{\mathbf{c}}), \tag{39}$$

and the expanded expressions of $\bar{\mathbf{c}}$ and $\tilde{\mathbf{c}}$ are given by (40) and (41) at the top of next page.

Obviously, if $\mathbf{\Psi}_{2,1}$ and $\mathbf{\Psi}_{4,3}$ are known, then the 2-D DOAs can be successfully estimated by performing EVD on $\mathbf{\Psi}_{2,1}$ and $\mathbf{\Psi}_{4,3}$, since the diagonal elements of $\mathbf{\Omega}_{2,1}$ and $\mathbf{\Omega}_{4,3}$ (which contain the 2-D DOA information) are the eigenvalues of $\mathbf{\Psi}_{2,1}$ and $\mathbf{\Psi}_{4,3}$. Unfortunately, $\mathbf{\Psi}_{2,1}$ and $\mathbf{\Psi}_{4,3}$ are unknown and cannot be obtained directly via (35) and (36), since $\mathbf{\Phi}_{1,2}(\mu)$ and $\mathbf{\Phi}_{3,4}(\mu)$ are also unknown. Hence we need to estimate $\mathbf{\Phi}_{1,2}(\mu)$ and $\mathbf{\Phi}_{3,4}(\mu)$ first. As some of the array antennas are calibrated, we construct the following optimization problems

$$\min_{\bar{\mathbf{c}},\mathbf{\Psi}_{2,1}} \left\|\mathbf{\Phi}_{1,2}(\mu)\hat{\mathbf{E}}_{s2} - \hat{\mathbf{E}}_{s1}\mathbf{\Psi}_{2,1}\right\|_F^2 \;\; s.\,t.\;\; \mathbf{W}_1\bar{\mathbf{c}} = \mathbf{1}_{P(Q-1)}, \tag{42}$$

$$\min_{\tilde{\mathbf{c}},\mathbf{\Psi}_{4,3}} \left\|\mathbf{\Phi}_{3,4}(\mu)\hat{\mathbf{E}}_{s4} - \hat{\mathbf{E}}_{s3}\mathbf{\Psi}_{4,3}\right\|_F^2 \;\; s.\,t.\;\; \mathbf{W}_2\tilde{\mathbf{c}} = \mathbf{1}_{Q(P-1)}, \tag{43}$$

where $\mathbf{W}_1$ and $\mathbf{W}_2$ are given by (44) and (45) at the top of the next page. In order to solve (42) and (43), we first minimize the cost function with respect to $\mathbf{\Psi}_{2,1}$ and $\mathbf{\Psi}_{4,3}$, whose closed-form solutions are

$$\hat{\mathbf{\Psi}}_{2,1} = \left(\hat{\mathbf{E}}_{s1}^H\hat{\mathbf{E}}_{s1}\right)^{-1}\hat{\mathbf{E}}_{s1}^H\mathbf{\Phi}_{1,2}(\mu)\hat{\mathbf{E}}_{s2}, \tag{46}$$

$$\hat{\mathbf{\Psi}}_{4,3} = \left(\hat{\mathbf{E}}_{s3}^H\hat{\mathbf{E}}_{s3}\right)^{-1}\hat{\mathbf{E}}_{s3}^H\mathbf{\Phi}_{3,4}(\mu)\hat{\mathbf{E}}_{s4}. \tag{47}$$

Consequently, the formulations (42) and (43) can be re-cast as

$$\min_{\bar{\mathbf{c}}} \left\|\mathbf{P}_{s1}\mathbf{\Phi}_{1,2}(\mu)\hat{\mathbf{E}}_{s2}\right\|_F^2 \;\; s.\,t.\;\; \mathbf{W}_1\bar{\mathbf{c}} = \mathbf{1}_{P(Q-1)}, \tag{48}$$

$$\min_{\tilde{\mathbf{c}}} \left\|\mathbf{P}_{s3}\mathbf{\Phi}_{3,4}(\mu)\hat{\mathbf{E}}_{s4}\right\|_F^2 \;\; s.\,t.\;\; \mathbf{W}_2\tilde{\mathbf{c}} = \mathbf{1}_{(P-1)Q}, \tag{49}$$

where $\mathbf{P}_{s1} = \mathbf{I}_{M-M_x} - \hat{\mathbf{E}}_{s1}(\hat{\mathbf{E}}_{s1}^H\hat{\mathbf{E}}_{s1})^{-1}\hat{\mathbf{E}}_{s1}^H$, and $\mathbf{P}_{s3} = \mathbf{I}_{M-M_y} - \hat{\mathbf{E}}_{s3}(\hat{\mathbf{E}}_{s3}^H\hat{\mathbf{E}}_{s3})^{-1}\hat{\mathbf{E}}_{s3}^H$.

With

$$\begin{aligned}\left\|\mathbf{P}_{s1}\mathbf{\Phi}_{1,2}(\mu)\hat{\mathbf{E}}_{s2}\right\|_F^2 &= \mathrm{Tr}\left(\hat{\mathbf{E}}_{s2}^H\mathbf{\Phi}_{1,2}^H(\mu)\mathbf{P}_{s1}^H\mathbf{P}_{s1}\mathbf{\Phi}_{1,2}(\mu)\hat{\mathbf{E}}_{s2}\right)\\ &= \mathrm{Tr}\left(\hat{\mathbf{E}}_{s2}^H\hat{\mathbf{E}}_{s2}\mathbf{\Phi}_{1,2}^H(\mu)\mathbf{P}_{s1}\mathbf{\Phi}_{1,2}(\mu)\right)\\ &= \bar{\mathbf{c}}^H\left(\hat{\mathbf{E}}_{s2}^H\hat{\mathbf{E}}_{s2}\odot\mathbf{P}_{s1}\right)\bar{\mathbf{c}},\end{aligned}$$

$$\begin{aligned}\left\|\mathbf{P}_{s3}\mathbf{\Phi}_{3,4}(\mu)\hat{\mathbf{E}}_{s4}\right\|_F^2 &= \mathrm{Tr}\left(\hat{\mathbf{E}}_{s4}^H\mathbf{\Phi}_{3,4}^H(\mu)\mathbf{P}_{s3}^H\mathbf{P}_{s3}\mathbf{\Phi}_{3,4}(\mu)\hat{\mathbf{E}}_{s4}\right)\\ &= \mathrm{Tr}\left(\hat{\mathbf{E}}_{s4}^H\hat{\mathbf{E}}_{s4}\mathbf{\Phi}_{3,4}^H(\mu)\mathbf{P}_{s3}\mathbf{\Phi}_{3,4}(\mu)\right)\\ &= \tilde{\mathbf{c}}^H\left(\hat{\mathbf{E}}_{s4}^H\hat{\mathbf{E}}_{s4}\odot\mathbf{P}_{s3}\right)\tilde{\mathbf{c}},\end{aligned}$$

(42) and (43) can be finally reformulated as

$$\min_{\bar{\mathbf{c}}}\; \bar{\mathbf{c}}^H\left(\hat{\mathbf{E}}_{s2}^H\hat{\mathbf{E}}_{s2}\odot\mathbf{P}_{s1}\right)\bar{\mathbf{c}} \;\; s.\,t.\;\; \mathbf{W}_1\bar{\mathbf{c}} = \mathbf{1}_{P(Q-1)}, \tag{50}$$

$$\min_{\tilde{\mathbf{c}}}\; \tilde{\mathbf{c}}^H\left(\hat{\mathbf{E}}_{s4}^H\hat{\mathbf{E}}_{s4}\odot\mathbf{P}_{s3}\right)\tilde{\mathbf{c}} \;\; s.\,t.\;\; \mathbf{W}_2\tilde{\mathbf{c}} = \mathbf{1}_{Q(P-1)}. \tag{51}$$

Define $\mathbf{\Gamma}_{1,2} = \hat{\mathbf{E}}_{s2}^H\hat{\mathbf{E}}_{s2}\odot\mathbf{P}_{s1}$, $\mathbf{\Gamma}_{3,4} = \hat{\mathbf{E}}_{s4}^H\hat{\mathbf{E}}_{s4}\odot\mathbf{P}_{s3}$, and by exploiting the well-known Lagrange multiplier method, we have

$$\hat{\bar{\mathbf{c}}} = \mathbf{\Gamma}_{1,2}^{-1}\mathbf{W}_1\left(\mathbf{W}_1^H\mathbf{\Gamma}_{1,2}^{-1}\mathbf{W}_1\right)^{-1}\mathbf{1}_{P(Q-1)}, \tag{52}$$

$$\hat{\tilde{\mathbf{c}}} = \mathbf{\Gamma}_{3,4}^{-1}\mathbf{W}_2\left(\mathbf{W}_2^H\mathbf{\Gamma}_{3,4}^{-1}\mathbf{W}_2\right)^{-1}\mathbf{1}_{Q(P-1)}. \tag{53}$$

With $\hat{\bar{\mathbf{c}}}$ and $\hat{\tilde{\mathbf{c}}}$, $\hat{\mathbf{\Phi}}_{1,2}(\mu)$ and $\hat{\mathbf{\Phi}}_{3,4}(\mu)$ are constructed as

$$\hat{\mathbf{\Phi}}_{1,2}(\mu) = \mathrm{diag}\{\hat{\bar{\mathbf{c}}}\}, \hat{\mathbf{\Phi}}_{\mathbf{3,4}}(\mu) = \mathrm{diag}\{\hat{\tilde{\mathbf{c}}}\}. \tag{54}$$

By further defining

$$\mathbf{\Upsilon}_a = [\hat{\mathbf{E}}_{s1}\;\hat{\mathbf{\Phi}}_{1,2}(\mu)\hat{\mathbf{E}}_{s2}]^H[\hat{\mathbf{E}}_{s1}\;\hat{\mathbf{\Phi}}_{1,2}(\mu)\hat{\mathbf{E}}_{s2}], \tag{55}$$

$$\mathbf{\Upsilon}_b = [\hat{\mathbf{E}}_{s3}\;\hat{\mathbf{\Phi}}_{3,4}(\mu)\hat{\mathbf{E}}_{s4}]^H[\hat{\mathbf{E}}_{s3}\;\hat{\mathbf{\Phi}}_{3,4}(\mu)\hat{\mathbf{E}}_{s4}], \tag{56}$$

and performing EVD on $\mathbf{\Upsilon}_a$ and $\mathbf{\Upsilon}_b$, we have

$$\mathbf{\Upsilon}_{\boldsymbol{a}} = \mathbf{U}_a\mathbf{\Lambda}_a\mathbf{U}_a^H, \;\; \mathbf{\Upsilon}_{\boldsymbol{b}} = \mathbf{U}_b\mathbf{\Lambda}_b\mathbf{U}_b^H, \tag{57}$$

where $\mathbf{U}_a$ and $\mathbf{U}_b$ are the $6K\times 6K$ eigenvectors of $\mathbf{\Upsilon}_{\boldsymbol{a}}$ and $\mathbf{\Upsilon}_{\boldsymbol{b}}$, respectively, while $\mathbf{\Lambda}_a$ and $\mathbf{\Lambda}_b$ are the $6K\times 6K$ diagonal matrices, whose diagonal elements correspond to the eigenvalues of $\mathbf{\Upsilon}_{\boldsymbol{a}}$ and $\mathbf{\Upsilon}_{\boldsymbol{b}}$, respectively.

$\mathbf{U}_a$ and $\mathbf{U}_b$ can be partitioned as

$$\mathbf{U}_a = \begin{bmatrix}\mathbf{U}_{a11} & \mathbf{U}_{a12}\\ \mathbf{U}_{a21} & \mathbf{U}_{a22}\end{bmatrix}, \mathbf{U}_b = \begin{bmatrix}\mathbf{U}_{b11} & \mathbf{U}_{b12}\\ \mathbf{U}_{b21} & \mathbf{U}_{b22}\end{bmatrix}, \tag{58}$$

and each submatrix has dimensions of $3K\times 3K$. Finally, $\mathbf{\Psi}_{2,1}$ and $\mathbf{\Psi}_{4,3}$ are estimated as

$$\hat{\mathbf{\Psi}}_{2,1} = -\mathbf{U}_{a12}\mathbf{U}_{a22}^{-1}, \;\; \hat{\mathbf{\Psi}}_{4,3} = -\mathbf{U}_{b12}\mathbf{U}_{b22}^{-1}. \tag{59}$$

Following the same estimation and matching procedure in [27] and [28] after conducting EVD on $\hat{\mathbf{\Psi}}_{2,1}$ and $\hat{\mathbf{\Psi}}_{3,4}$, we can obtain 2-D nominal DOAs of ID sources without ambiguities. Let $\upsilon_{1,3(k-1)+\tilde{l}}$ and $\upsilon_{2,3(k-1)+\tilde{l}}$ $(\tilde{l} = 1,2,3)$ denote the pair-matched eigenvalues of $\hat{\mathbf{\Psi}}_{2,1}$ and $\hat{\mathbf{\Psi}}_{4,3}$, which correspond to the estimates of $[\mathbf{\Omega}_{2,1}]_{k+(\tilde{l}-1)K,k+(\tilde{l}-1)K}$ and $[\mathbf{\Omega}_{4,3}]_{k+(\tilde{l}-1)K,k+(\tilde{l}-1)K}$, respectively. Finally, the nominal azimuth and elevation DOAs of the kth source are estimated as

$$\hat{\theta}_k = \frac{1}{3}\sum_{\tilde{l}=1}^{3}\tan^{-1}\left(\frac{\angle\upsilon_{1,3(k-1)+\tilde{l}}}{\angle\upsilon_{2,3(k-1)+\tilde{l}}}\right), \tag{60}$$

$$\hat{\phi}_k = \frac{1}{3}\sum_{\tilde{l}=1}^{3}\sin^{-1}\left(\frac{1}{u}\sqrt{\sum\nolimits_{p=1}^{2}\left(\angle\upsilon_{p,3(k-1)+\tilde{l}}\right)^2}\right), \tag{61}$$

where $k\in[1,K]$.

$$\bar{\mathbf{c}} = \Bigg[\underbrace{\mathbf{1}_P^T, \frac{\mu_{P+1}}{\mu_{M_x+P+1}}, \ldots, \frac{\mu_{M_x}}{\mu_{2M_x}}, \ldots, \mathbf{1}_P^T, \frac{\mu_{(Q-2)M_x+P+1}}{\mu_{(Q-1)M_x+P+1}}, \ldots, \frac{\mu_{(Q-1)M_x}}{\mu_{QM_x}}}_{1\times(Q-1)M_x}, \underbrace{\frac{1}{\mu_{QM_x+1}}, \ldots, \frac{1}{\mu_{QM_x+P}}}_{1\times P},$$
$$\underbrace{\frac{\mu_{(Q-1)M_x+P+1}}{\mu_{QM_x+P+1}}, \ldots, \frac{\mu_{QM_x}}{\mu_{(Q+1)M_x}}}_{1\times(M_x-P)}, \underbrace{\frac{\mu_{QM_x+1}}{\mu_{(Q+1)M_x+1}}, \ldots, \frac{\mu_{(M_y-1)M_x}}{\mu_{M_yM_x}}}_{1\times(M_y-Q-1)M_x}\Bigg]^T, \quad (40)$$

$$\tilde{\mathbf{c}} = \Bigg[\underbrace{\mathbf{1}_{P-1}^T, \frac{1}{\mu_{P+1}}, \frac{\mu_{P+1}}{\mu_{P+2}}, \ldots, \frac{\mu_{M_x-1}}{\mu_{M_x}}, \ldots, \mathbf{1}_{P-1}^T, \frac{1}{\mu_{(Q-1)M_x+P+1}}, \frac{\mu_{(Q-1)M_x+P+1}}{\mu_{(Q-1)M_x+P+2}}, \ldots, \frac{\mu_{QM_x-1}}{\mu_{QM_x}}}_{1\times(M_x-1)Q}, \underbrace{\frac{\mu_{QM_x+1}}{\mu_{QM_x+2}}, \ldots, \frac{\mu_{M_yM_x-1}}{\mu_{M_yM_x}}}_{1\times(M_x-1)(M_y-Q)}\Bigg]^T \quad (41)$$

$$\mathbf{W}_1 = \begin{bmatrix} \mathbf{I}_P & \mathbf{0}_{P\times(M_x-P)} & \mathbf{0}_{P\times(M_y-2)M_x} \\ \mathbf{0}_{P\times M_x} & \mathbf{I}_P & \mathbf{0}_{P\times(M_y-2)M_x-P} \\ \vdots & \vdots & \vdots \\ \mathbf{0}_{P\times(Q-2)M_x} & \mathbf{I}_P & \mathbf{0}_{P\times(M_y-Q+1)M_x-P} \end{bmatrix}, \quad (44)$$

$$\mathbf{W}_2 = \begin{bmatrix} \mathbf{I}_{P-1} & \mathbf{0}_{(P-1)\times(M_x-P)} & \mathbf{0}_{(P-1)\times(M_y-1)(M_x-1)} \\ \mathbf{0}_{(P-1)\times(M_x-1)} & \mathbf{I}_{P-1} & \mathbf{0}_{(P-1)\times[(M_y-1)(M_x-1)-P+1]} \\ \vdots & \vdots & \vdots \\ \mathbf{0}_{(P-1)\times(Q-1)(M_x-1)} & \mathbf{I}_{P-1} & \mathbf{0}_{(P-1)\times[(M_y-Q+1)(M_x-1)-P+1]} \end{bmatrix}. \quad (45)$$

B. Estimation of Gain-phase Perturbations and Angular Spreads

Based on $\hat{\bar{\mathbf{c}}}$ and $\hat{\tilde{\mathbf{c}}}$, we can further obtain estimation of the array gain-phase perturbations as

$$\hat{\mu}_{(Q+m)M_x+\rho} = \left\{\prod_{n=0}^{m} [\hat{\bar{\mathbf{c}}}]_{(Q-1-n)M_x+\rho}\right\}^{-1}, \quad m \in [0, M_y-Q-1], \rho \in [1, P], \quad (62)$$

$$\hat{\mu}_{\nu+mM_x} = \left\{\prod_{n=P+1}^{\nu} [\hat{\tilde{\mathbf{c}}}]_{n+m(M_x-1)-1}\right\}^{-1}, \quad \nu \in [P+1, M_x], m \in [0, Q-1]. \quad (63)$$

The detailed process of gain-phase perturbations estimation and calibration is illustrated in Fig. 3. Obviously, by using the $P \times Q$ well calibrated antennas as well as equations (62) and (63), we only obtain the estimate of gain-phase perturbations of antennas labeled as red and green circles. However, with such estimates, one can easily conclude that the gain-phase perturbations of the left antennas (labeled as blue circles) can be further estimated as

$$\hat{\mu}_{(Q+m)M_x+P+\rho} = \left\{\frac{\prod_{n=0}^{m} [\hat{\bar{\mathbf{c}}}]_{(Q-n-1)M_x+P+\rho}}{\hat{\mu}_{(Q-1)M_x+P+\rho}}\right\}^{-1}, \quad \rho \in [1, M_x-P,], m \in [0, M_y-Q-1]. \quad (64)$$

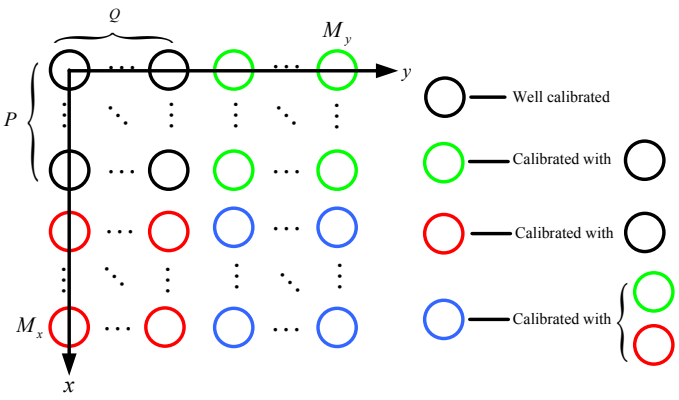

Fig. 3. Estimation process for array gain-phase perturbations, where black circles denote the well calibrated antennas, red and green circles the antennas calibrated with black circles, and blue ones the antennas calibrated with red or green circles.

As the gain-phase perturbations have been estimated, we first compensate them by

$$\breve{\mathbf{R}}_y = \hat{\mathbf{\Phi}}^{-1}(\mu)\left[\hat{\mathbf{R}}_y - \hat{\sigma}_n^2\mathbf{I}_M\right]\left(\hat{\mathbf{\Phi}}^H(\mu)\right)^{-1}, \quad (65)$$

where $\hat{\mathbf{\Phi}}(\mu)$ is the estimate of $\mathbf{\Phi}(\mu)$, and $\hat{\sigma}_n^2$ is the estimate of σ_n^2 obtained by averaging the smallest $M-3K$ eigenvalues of $\hat{\mathbf{R}}_y$.

Subsequently, we estimate $\mathbf{S}$ utilizing $\breve{\mathbf{R}}_y$ as

$$\hat{\mathbf{S}} = \left(\hat{\mathbf{A}}^H\hat{\mathbf{A}}\right)^{-1}\hat{\mathbf{A}}^H\breve{\mathbf{R}}_y\left(\hat{\mathbf{A}}\hat{\mathbf{A}}^H\right)^{-1}\hat{\mathbf{A}}, \quad (66)$$

where $\hat{\mathbf{A}}$ is the estimate of $\mathbf{A}(\theta, \phi)$. According to the expres-

Algorithm 1: Joint 2-D DOA, Gain-Phase Perturbation and Angular Spread Estimation

1: Calculate the sample covariance matrix $\hat{\mathbf{R}}_y$ according to (18) and perform EVD on $\hat{\mathbf{R}}_y$ to obtain signal subspace matrix $\hat{\mathbf{E}}_s$.
2: Form $\hat{\mathbf{E}}_{sl}, l \in [1,4]$ according to (31)$\sim$(34), and further construct $\mathbf{\Gamma}_{1,2} = \hat{\mathbf{E}}_{s2}^H \hat{\mathbf{E}}_{s2} \odot \mathbf{P}_{s1}$ and $\mathbf{\Gamma}_{3,4} = \hat{\mathbf{E}}_{s4}^H \hat{\mathbf{E}}_{s4} \odot \mathbf{P}_{s3}$.
3: Estimate $\hat{\bar{\mathbf{c}}}$ and $\hat{\tilde{\mathbf{c}}}$ based on (52) and (53), as well as $\hat{\mathbf{\Phi}}_{1,2}(\mu)$ and $\hat{\mathbf{\Phi}}_{3,4}(\mu)$ via (54).
4: Construct $\mathbf{\Upsilon}_a$ and $\mathbf{\Upsilon}_b$ according to (55) and (56), and then calculate $\hat{\mathbf{\Psi}}_{2,1}$ and $\hat{\mathbf{\Psi}}_{3,4}$ using (59).
5: Perform EVD on $\hat{\mathbf{\Psi}}_{2,1}$ and $\hat{\mathbf{\Psi}}_{3,4}$, and match their eigenvalues based on the method introduced in [20].
6: Estimate the nominal DOAs with (60) and (61), and gain-phase perturbations with (62)$\sim$(64).
7: Compensate the gain-phase perturbations to form $\breve{\mathbf{R}}_y$, and further obtain $\hat{\mathbf{S}}$ via (66).
8: Estimate angular spreads via (67) and (68).

sion of $\mathbf{S}$, σ_{θ_k} and σ_{ϕ_k} are respectively estimated as

$$\hat{\sigma}_{\theta_k} = \sqrt{\left[\hat{\mathbf{S}}\right]_{k+K,k+K} \Big/ \left[\hat{\mathbf{S}}\right]_{k,k}}, \quad k \in [1,K], \tag{67}$$

$$\hat{\sigma}_{\phi_k} = \sqrt{\left[\hat{\mathbf{S}}\right]_{k+2K,k+2K} \Big/ \left[\hat{\mathbf{S}}\right]_{k,k}}, \quad k \in [1,K]. \tag{68}$$

The proposed method for 2-D DOA estimation of ID sources in the presence of gain-phase perturbations is summarized in Algorithm 1, where $\hat{\chi}$ denotes the estimation result of χ with N samples.

Remark 1: The computational complexity of the proposed method mainly lies in the construction of $\hat{\mathbf{R}}_y$ and its EVD, the estimation of $\hat{\mathbf{\Psi}}_{2,1}$ and $\hat{\mathbf{\Psi}}_{4,3}$, and their EVDs, as well as the estimation of gain-phase perturbations, which in total requires multiplications of $O(M^2N + \frac{4}{3}M^3) + O(36(2M - M_x - M_y)K^2 + 144K^3) + O((M - M_x)^3 + (M - M_y)^3)$. Since M is far larger than K for a massive MIMO system, the complexity of the proposed method is close to $O\left(M^3\right)$ as $M \to \infty$, which is at the same level as that of the algorithm in [27].

Remark 2: It should be noted that the proposed method is designed for fully digital arrays, where each antenna element has its own Radio Frequency (RF) chain. However, in order to reduce the cost of RF chains in massive MIMO systems, hybrid antenna arrays are often adopted in practice. Under such a circumstance, one can first apply the preprocessing scheme [48], [49] to reconstruct the spatial covariance matrix as if a fully digital array is exploited, and then utilize the proposed method for 2-D DOA estimation, which implies that the proposed method is applicable to hybrid arrays with necessary adaptations.

Remark 3: The proposed method can be regarded as a modified version of ESPRIT based methods [10]-[15], [27]. Their differences are mainly reflected in the following two aspects: i) The existing ESPRIT based DOA estimation algorithms for massive MIMO systems are either established on the point source assumption or the ideal array model. In contrast, we take both the ID source model and the array gain-phase perturbations into account, and the developed modified ESPRIT method can yield a robust 2-D DOA estimation result for ID sources in the presence of unknown array gain-phase perturbations; ii) the influence of array gain-phase errors on the 2-D DOA estimation performance of ID sources in massive MIMO systems has not been analyzed and evaluated in existing ESPRIT based algorithms. In comparison, a detailed analysis is provided here on this point from both theoretical and simulation perspectives, which fills the gap in literature (see the next two sections for details).

IV. Performance Analysis and Cramér-Rao Bound

A. Required Number of Calibrated Antennas

It is clear that the effectiveness of the proposed method depends on calibration of part of the array antennas. More specifically, in order to yield meaningful solutions $\hat{\bar{\mathbf{c}}}$ and $\hat{\tilde{\mathbf{c}}}$ (as shown in (52) and (53)), the following inequalities must hold

$$P\left(Q-1\right) \geq 1, \;\; P \in \{1,2,\ldots,M_x\}, \tag{69}$$

$$Q\left(P-1\right) \geq 1, \;\; Q \in \{1,2,\ldots,M_y\}, \tag{70}$$

which means that at least 2×2 (i.e., $P \geq 2$, $Q \geq 2$) antennas must be well calibrated. Moreover, it is necessary for the $P \times Q$ calibrated antennas to be spatially continuous. Otherwise, the gain-phase perturbations cannot be obtained. In practice, calibrating spatially continuous antennas could be relatively easier and more convenient than calibrating the same number of antennas scattered around. Particularly, if the URA is fully calibrated, i.e., $P = M_x, Q = M_y$, the proposed method will be simplified to the ESPRIT-based in [27] and the only difference lies in their subarray division strategies.

B. Influence of Gain-Phase Perturbations on Estimation Accuracy

For simplicity, assume that the number of snapshots is sufficient and only $\mathbf{\Psi}_{2,1}$ is used for this analysis. Suppose that there exist array gain-phase perturbations, but one applies ESPRIT-based technique for 2-D DOA estimation without considering their influences. As a result, $\mathbf{\Psi}_{2,1}=\left(\mathbf{E}_{s1}^H\mathbf{E}_{s1}\right)^{-1}\mathbf{E}_{s1}^H\mathbf{\Phi}_{1,2}\left(\mu\right)\mathbf{E}_{s2}$ will deviate from its true value as $\bar{\mathbf{\Psi}}_{2,1}=\left(\mathbf{E}_{s1}^H\mathbf{E}_{s1}\right)^{-1}\mathbf{E}_{s1}^H\mathbf{E}_{s2}$. Define

$$\begin{aligned}\Delta\mathbf{\Psi}_{2,1}&=\mathbf{\Psi}_{2,1}-\bar{\mathbf{\Psi}}_{2,1}\\ &=\left(\mathbf{E}_{s1}^H\mathbf{E}_{s1}\right)^{-1}\mathbf{E}_{s1}^H\left(\mathbf{\Phi}_{1,2}\left(\mu\right)-\mathbf{I}_{M-M_x}\right)\mathbf{E}_{s2}.\end{aligned} \tag{71}$$

Obviously, $\Delta\mathbf{\Psi}_{2,1}$ will yield an error of eigenvalue

$$\begin{aligned}\Delta\upsilon_k &= \mathbf{q}_k\Delta\mathbf{\Psi}_{2,1}\mathbf{u}_k\\ &= \mathbf{q}_k\left(\mathbf{E}_{s1}^H\mathbf{E}_{s1}\right)^{-1}\mathbf{E}_{s1}^H\left(\mathbf{\Phi}_{1,2}\left(\mu\right)-\mathbf{I}_{M-M_x}\right)\mathbf{E}_{s2}\mathbf{u}_k\\ &= \sum_{m=1}^{M-M_x}\left[\bar{\mathbf{q}}\right]_m\left[\bar{\mathbf{c}}\right]_m\left[\bar{\mathbf{u}}^T\right]_m - \sum_{m=1}^{M-M_x}\left[\bar{\mathbf{q}}\right]_m\left[\bar{\mathbf{u}}^T\right]_m\\ &= \sum_{n=1}^{Q}\sum_{m=\bar{m}}^{nM_x}\left[\bar{\mathbf{q}}\right]\left(\left[\bar{\mathbf{c}}\right]_m-1\right)\left[\bar{\mathbf{u}}^T\right]_m\\ &= \upsilon_k\left(1-\bar{\rho}_c\right),\end{aligned}$$

where $\upsilon_k = \mathbf{q}_k\mathbf{\Psi}_{2,1}\mathbf{u}_k$, $\bar{\mathbf{q}} = \mathbf{q}_k\left(\mathbf{E}_{s1}^H\mathbf{E}_{s1}\right)^{-1}\mathbf{E}_{s1}^H$, $\bar{\mathbf{u}} = \mathbf{E}_{s2}\mathbf{u}_k$, and $\bar{\rho}_c = \sum_{m=1}^{M-M_x}\left[\bar{\mathbf{q}}\right]_m\left[\bar{\mathbf{u}}^T\right]_m/\upsilon_k$, $\bar{m}=(n-1)M_x+P+1$.

According to the relationship between the 2-D DOAs and the eigenvalues (polynomial roots), we have

$$\Delta\theta_k = \frac{1}{u\sin\phi_k\cos\theta_k}\mathrm{Im}\left(\Delta\upsilon_k/\upsilon_k\right), \tag{72}$$

$$\Delta\phi_k = \frac{1}{u\cos\phi_k\sin\theta_k}\mathrm{Im}\left(\Delta\upsilon_k/\upsilon_k\right). \tag{73}$$

It can be observed that $\Delta\theta_k = 0$ and $\Delta\phi_k = 0$ if the array is fully calibrated or the gain-phase perturbation in each antenna is identical. Meanwhile, the more number of antennas that are calibrated, the closer $\Delta\upsilon_k$ is to zero; the closer the gain-phase perturbations of two adjacent antennas are, the closer $\bar{\rho}_c$ is to one, and finally the closer $\Delta\theta_k$ and $\Delta\phi_k$ are to zeros. Unfortunately, the above mentioned conditions cannot be guaranteed in practice, and the perturbations between different antennas are typically different. Therefore, a direct application of ESPRIT-based estimators will produce a bias, regardless of the signal to noise ratio (SNR) and the number of snapshots. As a comparison, we estimate $\mathbf{\Phi}_{1,2}(\mu)$ first, and then obtain $\mathbf{\Psi}_{2,1}$ as $\mathbf{\Psi}_{2,1}{=}\left(\mathbf{E}_{s1}^H\mathbf{E}_{s1}\right)^{-1}\mathbf{E}_{s1}^H\mathbf{\Phi}_{1,2}(\mu)\,\mathbf{E}_{s2}$, which directly leads to the result that $\Delta\upsilon_k = 0$, $\Delta\theta_k = 0$, and $\Delta\phi_k = 0$. In other words, the performance of the existing ESPRIT-based estimators is affected by array gain-phase perturbations seriously (especially for large-scale antenna arrays), while the proposed method performs independent of such perturbations, which will also be validated by numerical simulations in Section V.

Remark 4: In case of finite number of snapshots, there exists another bias $\Delta\bar{\mathbf{\Psi}}_{2,1} = \hat{\mathbf{\Psi}}_{2,1} - \mathbf{\Psi}_{2,1}$, which will yield a new error of eigenvalue $\Delta\bar{\upsilon}_k = \hat{\upsilon}_k - \upsilon_k$. However, based on the central limit theorem, $\Delta\bar{\upsilon}_k$ will be small, provided that the number of snapshots is large enough.

C. Approximate Cramér-Rao Bound

The Cramér-Rao Bound (CRB) provides a lower bound on the covariance matrix of any unbiased estimator, which is obtained by taking the inverse of the Fisher information matrix (FIM). Define

$$\mathbf{z} = [\boldsymbol{\theta}^T, \boldsymbol{\varphi}^T, \boldsymbol{\sigma_\theta}^T, \boldsymbol{\sigma_\phi}^T, \boldsymbol{\sigma_\gamma}^T, \boldsymbol{\rho}^T, \boldsymbol{\varphi}^T, \boldsymbol{\sigma_s}^T]^T \tag{74}$$

as the vector of unknown parameters associated with our signal model, where $\boldsymbol{\theta} = [\theta_1, \ldots, \theta_K]^T$, $\boldsymbol{\phi} = [\phi_1, \ldots, \phi_K]^T$, $\boldsymbol{\sigma}_\theta = [\sigma_{\theta_1}^2, \sigma_{\theta_2}^2, \ldots, \sigma_{\theta_K}^2]^T$, $\boldsymbol{\sigma}_\phi = [\sigma_{\phi_1}^2, \sigma_{\phi_2}^2, \ldots, \sigma_{\phi_K}^2]^T$, $\boldsymbol{\sigma}_\gamma = [\sigma_{\gamma_1}^2, \sigma_{\gamma_2}^2, \ldots, \sigma_{\gamma_K}^2]^T$, $\boldsymbol{\sigma}_s = [\sigma_{s_1}^2, \sigma_{s_2}^2, \ldots, \sigma_{s_K}^2]^T$, and

$$\boldsymbol{\rho} = \{[\rho_{P+1}, \ldots, \rho_{M_x}, \ldots, \rho_{(Q-1)M_x+P+1}, \ldots, \rho_{Q_{M_x}}, \rho_{Q_{M_x+1}}, \ldots, \rho_M]^T\},$$

$$\boldsymbol{\varphi} = \{[\varphi_{P+1}, \ldots, \varphi_{M_x}, \ldots, \varphi_{(Q-1)M_x+P+1}, \ldots, \varphi_{Q_{M_x}}, \varphi_{Q_{M_x+1}}, \ldots, \varphi_M]^T\}.$$

The (l,h)th element of FIM $\mathbf{F}$ with covariance matrix $\mathbf{R}_y$ is given by

$$\mathbf{F}(l,h) = N\mathrm{Tr}\left\{\mathbf{R}_y^{-1}\frac{\partial\mathbf{R}_y}{\partial\varsigma_l}\mathbf{R}_y^{-1}\frac{\partial\mathbf{R}_y}{\partial\varsigma_h}\right\}, \tag{75}$$

whose matrix form is given in Appendix, and ς_l is the lth unknown parameter. Consequently, the CRBs of 2-D DOA estimations can be obtained by taking the inverse of $\mathbf{F}$, i.e.,

$$\mathrm{CRB}_\theta = \sqrt{\frac{1}{K}\sum\nolimits_{k=1}^{K}\left[\mathbf{F}^{-1}\right]_{kk}}, \tag{76}$$

$$\mathrm{CRB}_\phi = \sqrt{\frac{1}{K}\sum\nolimits_{k=K+1}^{2K}\left[\mathbf{F}^{-1}\right]_{kk}}. \tag{77}$$

Remark 5: The signal model used for approximate CRB derivation in [27] is different from that for algorithm derivation, and gain-phase perturbations are also not considered. In contrast, we take the gain-phase perturbations into account and the signal model used for the algorithm and CRB derivation is consistent, which indicates that the derived approximate CRB in this paper is more reasonable for performance assessment.

V. Simulations and Results

In this section, simulations are performed to demonstrate the effectiveness of the proposed method. The ESPRIT-based algorithm in [27] (named as ESPRIT-W), the ESPRIT-based algorithm in [27] combined with our gain-phase perturbations estimation and compensation result (named as ESPRIT-C), the efficient beamspace-based algorithm in [28] (named as Beamspace-W), the efficient beamspace-based algorithm in [28] combined with our gain-phase perturbations estimation and compensation result (named as Beamspace-C), as well as the approximate CRB obtained by the inverse of simplified FIM (the gain-phase perturbations are assumed to be known, which is just for the purpose of simplification since the whole FIM is hard to handle in the simulations) are selected for comparison. Meanwhile, the proposed method with perfect compensation (named as Proposed-P) is also simulated as a benchmark in some experiments. The number of antennas, the number of UEs and the number of multipaths are $M = 100$, $K = 2$ and $L_k = 50$, respectively, where $\sqrt{M} = M_x = M_y$ and $d = \lambda/2$. The signals transmitted from all UEs are BPSK modulated, and the basic spatial information of the two UEs are set to be $\{\theta_1, \phi_1, \sigma_{\theta_1}, \sigma_{\phi_1}, \sigma_{\gamma_1}\} = \{10^\circ, 20^\circ, 1^\circ, 1^\circ, 1\}$ and $\{\theta_2, \phi_2, \sigma_{\theta_2}, \sigma_{\phi_2}, \sigma_{\gamma_2}\} = \{30^\circ, 50^\circ, 1^\circ, 1^\circ, 1\}$, respectively. Except for the last simulation, the antennas in the first five columns are assumed to be well calibrated, whereas the gain and phase perturbations in other antennas are generated by [33], [45]

$$\rho_m = 1 + \sqrt{12}\sigma_\rho\xi_m,\ \psi_m = \sqrt{12}\sigma_\psi\zeta_m, \tag{78}$$

where ξ_m and ζ_m are independent and identically distributed random variables distributed uniformly over $[-0.5, 0.5]$, σ_ρ and σ_ψ are the standard deviations of ρ_m and ψ_m, respectively. The estimation performance is evaluated by the root mean square error (RMSE) from the results of 500 independent Monte-Carlo trials.

A. Performance versus Average Received SNR

In the first set of simulations, the impact of the average received SNR on the performance of different algorithms is evaluated, and the RMSE results are shown in Fig. 4. The

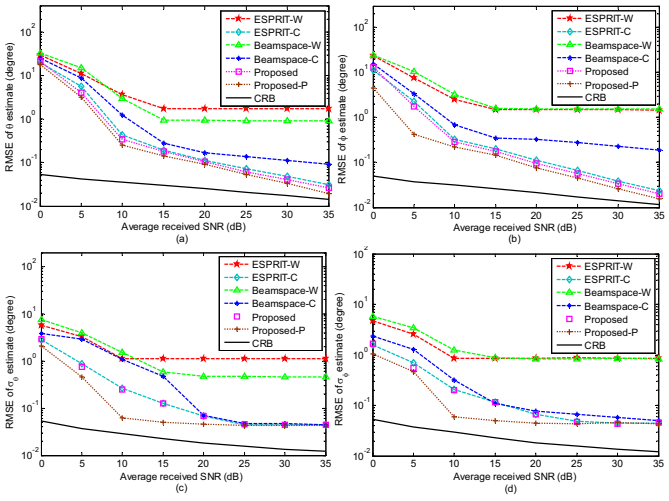

Fig. 4. RMSEs versus average received SNR, with $M = 100, N = 500$, $\sigma_\rho = 0.1$ and $\sigma_\psi = 20^\circ$. (a), (b), (c) and (d) correspond to the estimation of the nominal azimuth DOA, the nominal elevation DOA, the azimuth angular spread and the elevation angular spread, respectively.

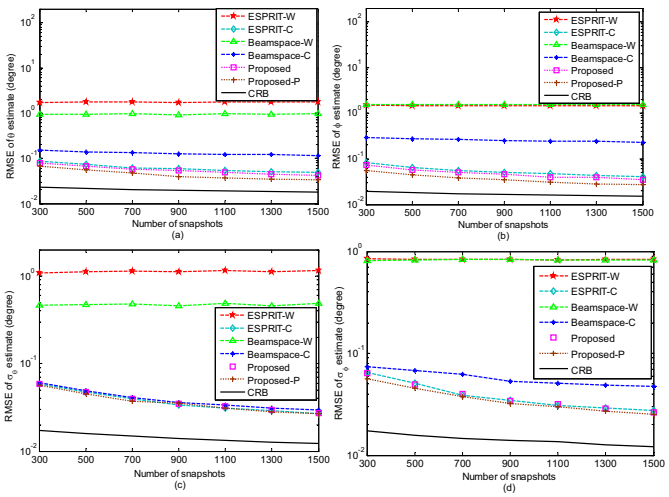

Fig. 5. RMSEs versus the number of snapshots, with $M = 100$, SNR=25dB, $\sigma_\rho = 0.1$ and $\sigma_\psi = 20^\circ$. (a), (b), (c) and (d) correspond to the estimation of the nominal azimuth DOA, the nominal elevation DOA, the azimuth angular spread and the elevation angular spread, respectively.

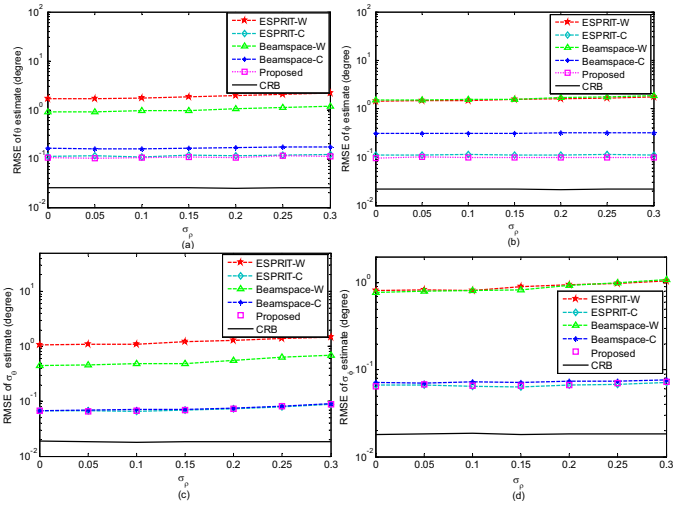

Fig. 6. RMSEs versus σ_ρ, with $M = 100$, $N = 500$, SNR=20dB, and $\sigma_\psi = 20^\circ$. (a), (b), (c) and (d) correspond to the estimation of the nominal azimuth DOA, the nominal elevation DOA, the azimuth angular spread and the elevation angular spread, respectively.

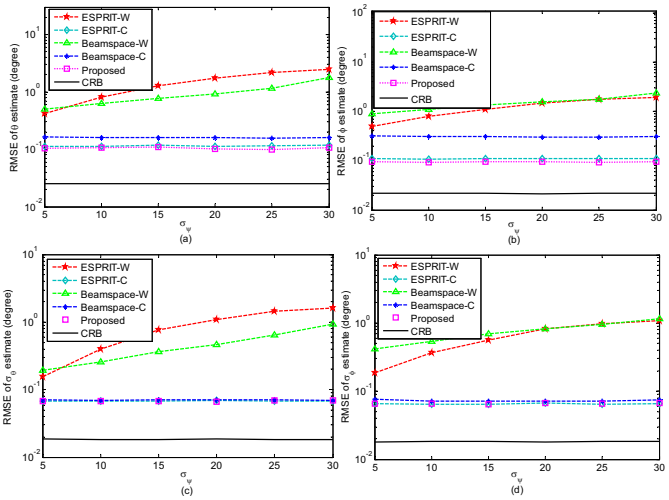

Fig. 7. RMSEs versus σ_ψ, with $M = 100$, $N = 500$, SNR=20dB, and $\sigma_\rho = 0.1$. (a), (b), (c) and (d) correspond to the estimation of the nominal azimuth DOA, the nominal elevation DOA, the azimuth angular spread and the elevation angular spread, respectively.

number of snapshots is set to 500, $\sigma_\rho = 0.1$, $\sigma_\psi = 20^\circ$, and the average received SNR varies from 0dB to 35dB. From Figs. 4(a)-4(d), it can be seen that the proposed method gives the best performance in the whole SNR region, and its RMSEs decrease rapidly as the average received SNR increases. In addition, it can be observed that direct application of the ESPRIT-based and the Beamspace-based algorithms (i.e., ESPRIT-W and Beamspace-W) suffer from serious performance degradation in the presence of array gain-phase perturbations. Moreover, by using the proposed calibrating strategy, their performance has been improved effectively. On the other hand, we also find that although both ESPRIT-C and Beamspace-C utilize the same gain-phase perturbation estimation and compensation mechanism, their nominal DOA estimation performance is still lower than the proposed method. This can be explained in that the proposed subarray division scheme can provide much more DOFs or elements of covariance matrix than that of the ESPRIT-based algorithm in [27] and the Beamspace-based algorithm in [28].

B. Performance versus the Number of Snapshots

In the second set of simulations, the performance of the proposed method is studied for different numbers of snapshots. The result is shown in Fig. 5, where SNR is fixed at 25dB, and the number of snapshots varies from 300 to 1500 with a step of 200. From Figs. 5(a)-5(d), it can be seen that the RMSEs of both nominal DOAs and their related angular spread estimations by the proposed method decrease monotonically with the number of snapshots. More specifically, for nominal DOAs estimation, the proposed method still leads the estimation performance, while for angular spreads estimation, the proposed method has almost the same performance as

ESPRIT-C and Beamspace-C. Meanwhile, we can also find that there is a gap between the RMSEs and the related CRBs. There are two possible reasons. Firstly, the estimation accuracy increases as the number of calibrated antennas increases, and when the array is fully calibrated, the RMSEs of the proposed method will be closer to CRBs, which can be verified from the simulation result of the Proposed-P method. Secondly, for a massive MIMO system, the array at the BS is equipped with a large number of antennas, and therefore, N is typically on the same order of magnitude as M. According to the general asymptotic theory [50], the sample covariance matrix is no more a good estimator of its true value under such circumstances, which directly yields that the RMSEs of the proposed method cannot follow the related CRBs very well. The problem of unbiased covariance matrix estimation for a massive MIMO system might be a topic of our further research.

C. Performance versus Gain and Phase Perturbations

Now the effect of gain perturbations and phase perturbations on the performance of the proposed method is examined. The SNR and the number of snapshots are set to 20dB and 500, respectively. In Fig. 6, $\sigma_\psi = 20^\circ$ and σ_ρ varies from 0 to 0.3, whereas in Fig. 7, $\sigma_\rho = 0.1$ and σ_ψ varies from 5° to 30°. From the simulation result, it can be seen that the performance of all the methods is influenced slightly by the gain perturbations, which is consistent with the observation in [51]. On the other hand, it can be observed that the performance of ESPRIT-W and Beamspace-W without calibration deteriorates greatly as phase perturbations increase. As a comparison, the proposed method performs almost independent of the gain-phase perturbations and can provide better estimation accuracy than the other considered algorithms.

D. Performance versus the Number of Calibrated Antennas

Finally, the RMSEs versus the number of calibrated antennas are provided. For simplicity, assume that L_c columns of antennas are calibrated, where L_c varies from 2 to 10. As shown in Fig. 8, the performance of all methods improves as the number of calibrated antennas increases. Meanwhile, the performance of the ESPRIT-W and Beamspace-W is affected by the array gain-phase perturbations seriously. Unless the array is fully calibrated (i.e., $L_c = 10$), their performance is not satisfactory at all. In contrast, by exploiting our calibration strategy, the proposed method as well as ESPRIT-C and Beamspace-C can provide a much better performance, provided that $L_c \geq 2$. In more detail, when $L_c \geq 5$, the RMSEs of both nominal DOAs and related angular spreads are lower than 10^{-1}, again demonstrating the effectiveness of the proposed method.

VI. Conclusion

In this paper, a new method for 2-D DOA estimation of ID sources has been proposed for massive MIMO systems in the presence of unknown gain-phase perturbations. In the proposed method, a shift invariance structure is first constructed

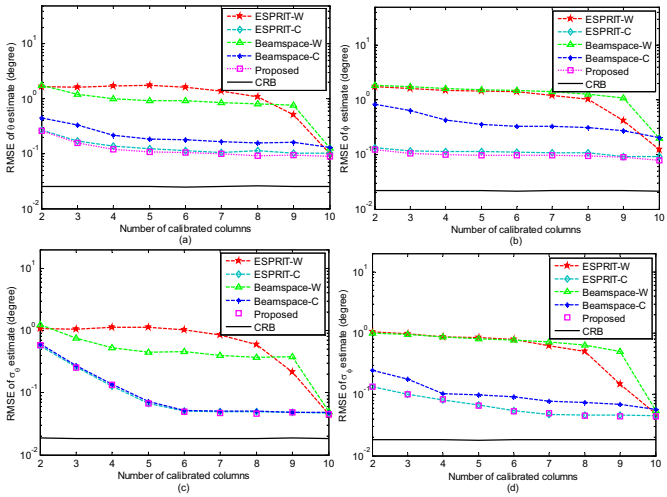

Fig. 8. RMSEs versus the number of calibrated columns of antenna array, with $M = 100$, $N = 500$, SNR=20dB, $\sigma_\rho = 0.1$ and $\sigma_\psi = 20^\circ$. (a), (b), (c) and (d) correspond to the estimation of the nominal azimuth DOA, the nominal elevation DOA, the azimuth angular spread and the elevation angular spread, respectively.

to obtain estimates of 2-D nominal DOAs and gain-phase perturbations in closed forms, and then estimation of angular spreads is achieved after compensating the estimated gain-phase perturbations. The approximate CRB for the studied partly calibrated URA is also derived, which matches better with the adopted approximate signal model. Through theoretical analysis and numerical simulations, it has been shown that the proposed method can provide not only improved estimation accuracy in a computationally efficient way, but also a performance almost independent of array gain-phase perturbations.

Derivation of the FIM $\mathbf{F}$

For simplicity, we construct $\mathbf{F}$ for $N = 1$. The results for $N > 1$ can be obtained by multiplying $\mathbf{F}$ by N. The partial derivative of the covariance matrix with azimuth angle θ_k is given by

$$\frac{\partial \mathbf{R}_y}{\partial \theta_k} = \mathbf{\Phi}\dot{\mathbf{A}}_{\theta_k}\mathbf{S}\mathbf{A}^H\mathbf{\Phi}^H + \mathbf{\Phi}\mathbf{A}\mathbf{S}\dot{\mathbf{A}}_{\theta_k}^H\mathbf{\Phi}^H, \tag{79}$$

where $\dot{\mathbf{A}}_{\theta_k} = \dot{\mathbf{A}}_\theta(\mathbf{e}_k\mathbf{e}_k^T + \mathbf{e}_{k+K}\mathbf{e}_{k+K}^T + \mathbf{e}_{k+2K}\mathbf{e}_{k+2K}^T)$ and $\dot{\mathbf{A}}_\theta = \sum_{k=1}^K \frac{\partial \mathbf{A}}{\partial \theta_k}$. Subsequently, we have

$$\begin{aligned}
&\mathrm{Tr}\left\{\mathbf{R}_y^{-1}\frac{\partial \mathbf{R}_y}{\partial \theta_k}\mathbf{R}_y^{-1}\frac{\partial \mathbf{R}_y}{\partial \theta_{\bar{k}}}\right\} \\
&= \mathrm{Tr}\Big\{\mathbf{R}_y^{-1}(\mathbf{\Phi}\dot{\mathbf{A}}_{\theta_k}\mathbf{S}\mathbf{A}^H\mathbf{\Phi}^H + \mathbf{\Phi}\mathbf{A}\mathbf{S}\dot{\mathbf{A}}_{\theta_k}^H\mathbf{\Phi}^H) \\
&\times\mathbf{R}_y^{-1}(\mathbf{\Phi}\dot{\mathbf{A}}_{\theta_{\bar{k}}}\mathbf{S}\mathbf{A}^H\mathbf{\Phi}^H + \mathbf{\Phi}\mathbf{A}\mathbf{S}\dot{\mathbf{A}}_{\theta_{\bar{k}}}^H\mathbf{\Phi}^H)\Big\} \\
&= 2\mathrm{Re}\Big\{\mathrm{Tr}\Big\{\mathbf{R}_y^{-1}\mathbf{\Phi}\dot{\mathbf{A}}_{\theta_k}\mathbf{S}\mathbf{A}^H\mathbf{\Phi}^H\mathbf{R}_y^{-1}\mathbf{\Phi}\dot{\mathbf{A}}_{\theta_{\bar{k}}}\mathbf{S}\mathbf{A}^H\mathbf{\Phi}^H \\
&\quad + \mathbf{R}_y^{-1}\mathbf{\Phi}\dot{\mathbf{A}}_{\theta_k}\mathbf{S}\mathbf{A}^H\mathbf{\Phi}^H\mathbf{R}_y^{-1}\mathbf{\Phi}\mathbf{A}\mathbf{S}\dot{\mathbf{A}}_{\theta_{\bar{k}}}^H\mathbf{\Phi}^H\Big\}\Big\} \\
&= 2\mathrm{Re}\left\{\sum_{i=1}^{9}(\bar{\mathbf{A}}_i(k,\bar{k}) \odot \bar{\mathbf{A}}_i^T(k,\bar{k})) + (\bar{\mathbf{B}}_i(k,\bar{k}) \odot \bar{\mathbf{C}}_i^T(k,\bar{k}))\right\},
\end{aligned}$$

where $k, \bar{k} \in [1, K]$, $\bar{\mathbf{A}} = \mathbf{S}\mathbf{A}^H\mathbf{\Phi}^H\mathbf{R}_y^{-1}\mathbf{\Phi}\dot{\mathbf{A}}_\theta \in \mathbb{C}^{3K\times 3K}$, $\bar{\mathbf{B}} = \mathbf{S}\mathbf{A}^H\mathbf{\Phi}^H\mathbf{R}_y^{-1}\mathbf{\Phi}\mathbf{A}\mathbf{S} \in \mathbb{C}^{3K\times 3K}$, $\bar{\mathbf{C}} = \dot{\mathbf{A}}_\theta^H\mathbf{\Phi}^H\mathbf{R}_y^{-1}\dot{\mathbf{A}}_\theta\mathbf{\Phi} \in \mathbb{C}^{3K\times 3K}$, $\bar{\mathbf{A}}_i$, $\bar{\mathbf{B}}_i$, $\bar{\mathbf{C}}_i$ are the ith block

of $\bar{\mathbf{A}}$, $\bar{\mathbf{B}}$ and $\bar{\mathbf{C}}$, respectively. Taking $\bar{\mathbf{A}}$ as an example, its various blocks $\bar{\mathbf{A}}_i \in \mathbb{C}^{K\times K}$, $i \in [1,9]$, are given by

$$\bar{\mathbf{A}} = \begin{bmatrix} \bar{\mathbf{A}}_1 & \bar{\mathbf{A}}_2 & \bar{\mathbf{A}}_3 \\ \bar{\mathbf{A}}_4 & \bar{\mathbf{A}}_5 & \bar{\mathbf{A}}_6 \\ \bar{\mathbf{A}}_7 & \bar{\mathbf{A}}_8 & \bar{\mathbf{A}}_9 \end{bmatrix}.$$

Consequently, the Fisher information matrix $\mathbf{F}$ with respect to azimuth angle θ is given by

$$\mathbf{F}_{\theta\theta} = 2\mathrm{Re}\left\{\sum_{i=1}^{9}\left(\bar{\mathbf{A}}_i \odot \bar{\mathbf{A}}_i^T + \bar{\mathbf{B}}_i \odot \bar{\mathbf{C}}_i^T\right)\right\}. \tag{80}$$

Similarly, the partial derivatives of the covariance matrix with other unknown parameters are given by

$$\begin{aligned}
\frac{\partial \mathbf{R}_y}{\partial \phi_k} &= \mathbf{\Phi}\dot{\mathbf{A}}_{\phi_k}\mathbf{S}\mathbf{A}^H\mathbf{\Phi}^H + \mathbf{\Phi}\mathbf{A}\mathbf{S}\dot{\mathbf{A}}_{\phi_k}^H\mathbf{\Phi}^H,\\
\frac{\partial \mathbf{R}_y}{\partial \rho_m} &= \dot{\mathbf{\Phi}}_{\rho_m}\mathbf{A}\mathbf{S}\mathbf{A}^H\mathbf{\Phi}^H + \mathbf{\Phi}\mathbf{A}\mathbf{S}\mathbf{A}^H\dot{\mathbf{\Phi}}_{\rho_m}^H,\\
\frac{\partial \mathbf{R}_y}{\partial \psi_m} &= \dot{\mathbf{\Phi}}_{\psi_m}\mathbf{A}\mathbf{S}\mathbf{A}^H\mathbf{\Phi}^H + \mathbf{\Phi}\mathbf{A}\mathbf{S}\mathbf{A}^H\dot{\mathbf{\Phi}}_{\psi_m}^H,\\
\frac{\partial \mathbf{R}_y}{\partial \sigma_{\theta_k}^2} &= \mathbf{\Phi}\mathbf{A}\dot{\mathbf{S}}_{\sigma_{\theta_k}}\mathbf{A}^H\mathbf{\Phi}^H, \frac{\partial \mathbf{R}_y}{\partial \sigma_{\phi_k}^2} = \mathbf{\Phi}\mathbf{A}\dot{\mathbf{S}}_{\sigma_{\phi_k}}\mathbf{A}^H\mathbf{\Phi}^H,\\
\frac{\partial \mathbf{R}_y}{\partial \sigma_{\gamma_k}^2} &= \mathbf{\Phi}\mathbf{A}\dot{\mathbf{S}}_{\sigma_{\gamma_k}}\mathbf{A}^H\mathbf{\Phi}^H, \frac{\partial \mathbf{R}_y}{\partial \sigma_{s_k}^2} = \mathbf{\Phi}\mathbf{A}\dot{\mathbf{S}}_{\sigma_{s_k}}\mathbf{A}^H\mathbf{\Phi}^H,
\end{aligned}$$

where

$$\begin{aligned}
\dot{\mathbf{A}}_{\phi_k} &= \dot{\mathbf{A}}_{\phi}(\mathbf{e}_k\mathbf{e}_k^T + \mathbf{e}_{k+K}\mathbf{e}_{k+K}^T + \mathbf{e}_{k+2K}\mathbf{e}_{k+2K}^T),\\
\dot{\mathbf{S}}_{\sigma_{\theta_k}} &= \dot{\mathbf{S}}_{\sigma_\theta}\mathbf{e}_{k+K}\mathbf{e}_{k+K}^T, \dot{\mathbf{S}}_{\sigma_{\phi_k}} = \dot{\mathbf{S}}_{\sigma_\phi}\mathbf{e}_{k+2K}\mathbf{e}_{k+2K}^T,\\
\dot{\mathbf{S}}_{\sigma_{s_k}} &= \dot{\mathbf{S}}_{\sigma_s}(\mathbf{e}_k\mathbf{e}_k^T + \mathbf{e}_{k+K}\mathbf{e}_{k+K}^T + \mathbf{e}_{k+2K}\mathbf{e}_{k+2K}^T),\\
\dot{\mathbf{S}}_{\sigma_{\gamma_k}} &= \dot{\mathbf{S}}_{\sigma_\gamma}(\mathbf{e}_k\mathbf{e}_k^T + \mathbf{e}_{k+K}\mathbf{e}_{k+K}^T + \mathbf{e}_{k+2K}\mathbf{e}_{k+2K}^T),\\
\dot{\mathbf{\Phi}}_{\rho_m} &= \dot{\mathbf{\Phi}}_{\rho}\mathbf{e}_m\mathbf{e}_m^T, \dot{\mathbf{\Phi}}_{\psi_m} = \dot{\mathbf{\Phi}}_{\psi}\mathbf{e}_m\mathbf{e}_m^T,
\end{aligned}$$

and $\dot{\mathbf{A}}_\phi = \sum_{k=1}^K \frac{\partial \mathbf{A}}{\partial \phi_k}$, $\dot{\mathbf{\Phi}}_\rho = \sum_{m=1}^M \frac{\partial \mathbf{\Phi}}{\partial \rho_m}$, $\dot{\mathbf{\Phi}}_\psi = \sum_{m=1}^M \frac{\partial \mathbf{\Phi}}{\partial \psi_m}$, $\dot{\mathbf{S}}_{\sigma_\theta} = \sum_{k=1}^K \frac{\partial \mathbf{S}}{\partial \sigma_{\theta_k}^2}$, $\dot{\mathbf{S}}_{\sigma_\phi} = \sum_{k=1}^K \frac{\partial \mathbf{S}}{\partial \sigma_{\phi_k}^2}$, $\dot{\mathbf{S}}_{\sigma_s} = \sum_{k=1}^K \frac{\partial \mathbf{S}}{\partial \sigma_{s_k}^2}$.

Following a similar procedure as in calculating $\mathbf{F}_{\theta\theta}$, we obtain the other blocks of $\mathbf{F}$. For example, the expressions of $\mathbf{F}_{\phi\phi}$, $\mathbf{F}_{\rho\rho}$, $\mathbf{F}_{\psi\psi}$, $\mathbf{F}_{\sigma_\theta\sigma_\theta}$, $\mathbf{F}_{\sigma_\phi\sigma_\phi}$ and $\mathbf{F}_{\sigma_s\sigma_s}$ are respectively given by

$$\mathbf{F}_{\phi\phi} = 2\mathrm{Re}\left\{\sum_{i=1}^{9}\left(\bar{\mathbf{D}}_i \odot \bar{\mathbf{D}}_i^T + \bar{\mathbf{B}}_i \odot \bar{\mathbf{E}}_i^T\right)\right\}, \tag{81}$$

$$\mathbf{F}_{\rho\rho} = 2\mathrm{Re}\left\{\tilde{\mathbf{H}}[\bar{\mathbf{F}} \odot \bar{\mathbf{F}}^T + \bar{\mathbf{G}} \odot \bar{\mathbf{H}}^T]\tilde{\mathbf{H}}^T\right\}, \tag{82}$$

$$\mathbf{F}_{\psi\psi} = 2\mathrm{Re}\left\{\tilde{\mathbf{H}}[\bar{\mathbf{I}} \odot \bar{\mathbf{I}}^T + \bar{\mathbf{J}} \odot \bar{\mathbf{H}}^T]\tilde{\mathbf{H}}^T\right\}, \tag{83}$$

$$\mathbf{F}_{\sigma_\theta\sigma_\theta} = 2\mathrm{Re}\left\{\bar{\mathbf{K}}_5 \odot \bar{\mathbf{K}}_5^T\right\}, \tag{84}$$

$$\mathbf{F}_{\sigma_\phi\sigma_\phi} = 2\mathrm{Re}\left\{\bar{\mathbf{L}}_9 \odot \bar{\mathbf{L}}_9^T\right\}, \tag{85}$$

$$\mathbf{F}_{\sigma_s\sigma_s} = 2\mathrm{Re}\left\{\sum_{i=1}^{9}\bar{\mathbf{M}}_i \odot \bar{\mathbf{M}}_i^T\right\}, \tag{86}$$

where

$$\begin{aligned}
\bar{\mathbf{D}} &= \mathbf{S}\mathbf{A}^H\mathbf{\Phi}^H\mathbf{R}_y^{-1}\mathbf{\Phi}\dot{\mathbf{A}}_\phi, \bar{\mathbf{E}} = \dot{\mathbf{A}}_\phi^H\mathbf{\Phi}^H\mathbf{R}_y^{-1}\dot{\mathbf{A}}_\phi\mathbf{\Phi},\\
\bar{\mathbf{F}} &= \mathbf{A}\mathbf{S}\mathbf{A}^H\mathbf{R}_y^{-1}\dot{\mathbf{\Phi}}_\rho, \bar{\mathbf{G}} = \dot{\mathbf{\Phi}}_\rho^H\mathbf{R}_y^{-1}\dot{\mathbf{\Phi}}_\rho,\\
\bar{\mathbf{H}} &= \mathbf{A}\mathbf{S}\mathbf{A}^H\mathbf{\Phi}^H\mathbf{R}_y^{-1}\mathbf{\Phi}\mathbf{A}\mathbf{S}\mathbf{A}^H, \bar{\mathbf{I}} = \mathbf{A}\mathbf{S}\mathbf{A}^H\mathbf{R}_y^{-1}\dot{\mathbf{\Phi}}_\psi,\\
\bar{\mathbf{J}} &= \dot{\mathbf{\Phi}}_\psi^H\mathbf{R}_y^{-1}\dot{\mathbf{\Phi}}_\psi, \bar{\mathbf{K}} = \mathbf{A}^H\mathbf{\Phi}^H\mathbf{R}_y^{-1}\mathbf{\Phi}\mathbf{A}\dot{\mathbf{S}}_{\sigma_\theta},\\
\bar{\mathbf{L}} &= \mathbf{A}^H\mathbf{\Phi}^H\mathbf{R}_y^{-1}\mathbf{\Phi}\mathbf{A}\dot{\mathbf{S}}_{\sigma_\phi}, \bar{\mathbf{M}} = \mathbf{A}^H\mathbf{\Phi}^H\mathbf{R}_y^{-1}\mathbf{\Phi}\mathbf{A}\dot{\mathbf{S}}_{\sigma_s},
\end{aligned}$$

and

$$\tilde{\mathbf{H}} = \mathrm{blkdiag}\left([\tilde{\mathbf{H}}_1 \ldots \tilde{\mathbf{H}}_Q \ \ \mathbf{I}_{(M_y-Q)M_x}]\right),$$

$$\tilde{\mathbf{H}}_1 = \ldots = \tilde{\mathbf{H}}_Q = \left[\mathbf{0}_{(M_x-P)\times P} \ \ \mathbf{I}_{M_x-P}\right].$$

As a result, the matrix form of $\mathbf{F}$ is expressed as

$$\mathbf{F} = \begin{bmatrix}
\mathbf{F}_{\theta\theta} & \mathbf{F}_{\theta\phi} & \mathbf{F}_{\theta\sigma_\theta} & \mathbf{F}_{\theta\sigma_\phi} & \mathbf{F}_{\theta\sigma_\gamma} & \mathbf{F}_{\theta\rho} & \mathbf{F}_{\theta\psi} & \mathbf{F}_{\theta\sigma_s}\\
\mathbf{F}_{\phi\theta} & \mathbf{F}_{\phi\phi} & \mathbf{F}_{\phi\sigma_\theta} & \mathbf{F}_{\phi\sigma_\phi} & \mathbf{F}_{\phi\sigma_\gamma} & \mathbf{F}_{\phi\rho} & \mathbf{F}_{\phi\psi} & \mathbf{F}_{\phi\sigma_s}\\
\mathbf{F}_{\sigma_\theta\theta} & \mathbf{F}_{\sigma_\theta\phi} & \mathbf{F}_{\sigma_\theta\sigma_\theta} & \mathbf{F}_{\sigma_\theta\sigma_\phi} & \mathbf{F}_{\sigma_\theta\sigma_\gamma} & \mathbf{F}_{\sigma_\theta\rho} & \mathbf{F}_{\sigma_\theta\psi} & \mathbf{F}_{\sigma_\theta\sigma_s}\\
\mathbf{F}_{\sigma_\phi\theta} & \mathbf{F}_{\sigma_\phi\phi} & \mathbf{F}_{\sigma_\phi\sigma_\theta} & \mathbf{F}_{\sigma_\phi\sigma_\phi} & \mathbf{F}_{\sigma_\phi\sigma_\gamma} & \mathbf{F}_{\sigma_\phi\rho} & \mathbf{F}_{\sigma_\phi\psi} & \mathbf{F}_{\sigma_\phi\sigma_s}\\
\mathbf{F}_{\sigma_\gamma\theta} & \mathbf{F}_{\sigma_\gamma\phi} & \mathbf{F}_{\sigma_\gamma\sigma_\theta} & \mathbf{F}_{\sigma_\gamma\sigma_\phi} & \mathbf{F}_{\sigma_\gamma\sigma_\gamma} & \mathbf{F}_{\sigma_\gamma\rho} & \mathbf{F}_{\sigma_\gamma\psi} & \mathbf{F}_{\sigma_\gamma\sigma_s}\\
\mathbf{F}_{\rho\theta} & \mathbf{F}_{\rho\phi} & \mathbf{F}_{\rho\sigma_\theta} & \mathbf{F}_{\rho\sigma_\phi} & \mathbf{F}_{\rho\sigma_\gamma} & \mathbf{F}_{\rho\rho} & \mathbf{F}_{\rho\psi} & \mathbf{F}_{\rho\sigma_s}\\
\mathbf{F}_{\psi\theta} & \mathbf{F}_{\psi\phi} & \mathbf{F}_{\psi\sigma_\theta} & \mathbf{F}_{\psi\sigma_\phi} & \mathbf{F}_{\psi\sigma_\gamma} & \mathbf{F}_{\psi\rho} & \mathbf{F}_{\psi\psi} & \mathbf{F}_{\psi\sigma_s}\\
\mathbf{F}_{\sigma_s\theta} & \mathbf{F}_{\sigma_s\phi} & \mathbf{F}_{\sigma_s\sigma_\theta} & \mathbf{F}_{\sigma_s\sigma_\phi} & \mathbf{F}_{\sigma_s\sigma_\gamma} & \mathbf{F}_{\sigma_s\rho} & \mathbf{F}_{\sigma_s\psi} & \mathbf{F}_{\sigma_s\sigma_s}
\end{bmatrix}.$$

This ends the derivation related to the matrix form of $\mathbf{F}$. □

REFERENCES

[1] M. Sakai, K. Kamohara, H. Iura, *et al.*, "Experimental field trials on MU-MIMO transmissions for high SHF wide-band massive MIMO in 5G," *IEEE Trans. Wireless Commun.*, vol. 19, no. 4, pp. 2196-2207, Apr. 2020.

[2] E. G. Larsson, O. Edfors, F. Tufvesson, and T. L. Marzetta, "Massive MIMO for next generation wireless systems," *IEEE Commun. Mag.*, vol. 52, no. 2, pp. 186-195, Feb. 2014.

[3] Z. Chen, F. Sohrabi and W. Yu, "Multi-cell sparse activity detection for massive random access: massive MIMO versus cooperative MIMO," *IEEE Trans. Wireless Commun.*, vol. 18, no. 8, pp. 4060-4074, Aug. 2019

[4] L. Dai, B. Wang, M. Peng, and S. Chen, "Hybird precoding-based millimeter-wave massive MIMO-NOMA with simultaneous wireless information and power transfer," *IEEE J. Sel. Areas Commun.*, vol. 37, no. 1, pp. 131-141, Jan. 2019.

[5] B. L. Ng, Y. Kim, J. Lee, *et al.*, "Fulfilling the promise of massive MIMO with 2D active antenna array," in *Proc. IEEE Globecom Workshops*, Anaheim, USA, Dec. 2012, pp. 691-696.

[6] T. T. Do, H. Q. Ngo, T. Q. Duong, *et al.*, "Massive MIMO pilot retransmission strategies for robustification against jamming," *IEEE Wireless Commun. Lett.*, vol. 6, no. 1, pp. 58-61, Feb. 2017.

[7] T. Ahmed, X. Zhang, and W. U. Hassan, "A higher-order propagator method for 2D-DOA estimation in massive MIMO systems," *IEEE Commun. Lett.*, vol. 24, no. 3, pp. 543-547, Mar. 2020.

[8] L. Liu, Y. Li, and J. Zhang, "DoA estimation and achievable rate analysis for 3D millimeter wave massive MIMO systems," in *Proc. IEEE 15th Int. Workshop Signal Process. Adv. Wireless Commun. (SPAWC)*, Toronto, ON, Canada, Jun. 2014, pp. 6-10.

[9] F. Wen and C. Liang, "Improved tensor-MODE based direction-of-arrival estimation for massive MIMO systems," *IEEE Commun. Lett.*, vol. 19, no. 12, pp. 2182-2185, Dec. 2015.

[10] R. Shafin, L. Liu, J. Zhang, and Y. C. Wu, "DoA estimation and capacity analysis for 3-D millimeter wave massive-MIMO/FD-MIMO OFDM systems," *IEEE Trans. Wireless Commun.*, vol. 15, no. 10, pp. 6963-6977, Oct. 2016.

[11] R. Shafin, L. Liu, Y. Li, *et al.*, "Angle and delay estimation for 3-D massive MIMO/FD-MIMO systems based on parametric channel modeling," *IEEE Trans. Wireless Commun.*, vol. 16, no. 8, pp. 5370-5383, Aug. 2017.

[12] R. Shafin and L. Liu, "Multi-cell multi-user massive FD-MIMO: Downlink precoding and throughput analysis," *IEEE Trans. Wireless Commun.*, vol. 18, no. 1, pp. 487-502, Jan. 2019.

[13] R. Shafin, M. Jiang, S. Ma, *et al.*, "Joint parametric channel estimation and performance characterization for 3D massive MIMO OFDM systems," in *Proc. 2018 IEEE Int. Conf. Commun. (ICC)*, Kansas City, MO, USA, May 2018, pp. 1-6.
[14] R. Shafin, L. Liu, and J. Zhang, "DoA estimation and RMSE characterization for 3D massive-MIMO/FD-MIMO OFDM system," in *Proc. 2015 IEEE Global Commun. (GLOBECOM)*, San Diego, CA, USA, Dec. 2015, pp. 1-6.
[15] R. Shafin, L. Liu, and J. C. Zhang, "DoA estimation and capacity analysis for 3D massive-MIMO/FD-MIMO OFDM system," in *Proc. 2015 IEEE Global Conf. Signal and Information Process. (GlobalSIP)*, Orlando, FL, USA, Dec. 2015, pp. 181-184.
[16] F. Shu, Y. Qin, T. Liu, *et al.*, "Low-complexity and high-resolution DOA estimation for hybird analog and digital maasive MIMO receive array," *IEEE Trans. Commun*., vol. 66, no. 6, pp. 2487-2501, Jun. 2018.
[17] L. Hachad, O. Cherrak, H. Ghennioui, *et al.*, "DOA estimation based on time-frequency MUSIC application to massive MIMO systems," in *Proc. Advanced Tech. Signal and Image Process*., Fez, Morroco, May 2017, pp. 22-24.
[18] P. Zetterberg and B. Ottersten, "The spectrum efficiency of a base station antenna array system for spatially selective transmission," *IEEE Trans. Veh. Technol*., vol. 44, no. 3, pp. 651-660, Aug. 1995.
[19] C. Liu, Y. Liu, and Z. Qiu, "Direction of arrival estimation for coherently distributed sources in 2D massive MIMO systems," in *Proc. Compu. Commun*., Chengdu, China, Oct. 2016, pp. 1942-1946.
[20] Y. Zhou, Z. Fei, S. Yang, *et al.*, "Joint angle estimation and signal reconstruction for coherently distributed sources in massive MIMO systems based on 2-D unitary ESPRIT," *IEEE Access*, vol. 5, pp. 9632-9646, 2017.
[21] L. Wan, G. Han, J. Jiang, *et al.*, "DOA estimation for coherently distributed sources considering circular and noncircular signals in massive MIMO systems," *IEEE Syst. J.*, vol. 11, no. 1, pp. 41-49, Mar. 2017.
[22] Y. Liu, L. Hou, Q. Shen, *et al.*, "Beamspace U-ESPRIT DOA estimation algorithm of coherently distributed sources in massive MIMO systems," in *Proc. Advanced Computational Intell*., Dali, China, Aug. 2020, pp. 126-132.
[23] Y. Tian, H. Yue, and X. Rong, "Multi-parameters estimation of coherently distributed sources under coexistence of circular and noncircular signals," *IEEE Commun. Lett*., vol. 24, no. 6, pp. 1254-1257, Jun. 2020.
[24] Y. Meng, P. Stoica, and K. Wong, "Estimation of the directions of arrival of spatially dispersed signals in array processing," in *Proc. IEE Radar, Sonar Navigat*., vol. 143, no. 1, pp. 1-9, Feb. 1996.
[25] H. Boujemaa, "Extension of COMET algorithm to multiple diffuse source localization in zaimuth and elevation," *Eur. Trans. Telecommun*., vol. 16, no. 6, pp. 557-566, Nov./Dec. 2005.
[26] A. Zoubir, Y. Wang, and P. Chargé, "Efficient subspace-based estimator for localization of multiple incoherently distributed sources," *IEEE Trans. Signal Process*., vol. 56, no. 2, pp. 532-542, Feb. 2008.
[27] A. Hu, T. Lv, H. Cao, *et al.*, "An ESPRIT-based approach for 2-D localization of incoherently distributed sources in massive MIMO systems," *IEEE J. Sel. Topics Signal Process.*, vol. 8, no. 5, pp. 996-1011, Oct. 2014.
[28] Z. Zheng, W. Wang, H. Meng, *et al.*, "Efficient beanspace-based algorithm for two-dimensional DOA estimation of incoherently distributed sources in massive MIMO systems," *IEEE Trans. Veh. Technol*., vol. 67, no. 12, pp. 11776-11789, Dec. 2018.
[29] T. Lv, F. Tan, H. Gao, and S. Yang, "A beamspace approach for 2-D localization of incoherently distributed sources in massive MIMO systems," *Signal Process*., vol. 121, pp. 30-45, 2016.
[30] L. Cheng, Y. C. Wu, J. Zhang, and L. Liu, "Subspace identification for DOA estimation in massive/full-dimension MIMO systems: Bad data mitigation and automatic source enumeration," *IEEE Trans. Signal Process*., vol. 63, no. 22, pp. 5897-5909, Nov. 2015.
[31] L. Qin, C. Li, Y. Du, and B. Li, "DOA estimation and mutual coupling calibration algoithm for array in plasma environment," *IEEE Trans. Plasma Sci*., vol. 48, no. 6, Jun. 2020.
[32] M. Jansson, A. L. Swindlehurst, and B. Ottersten, "Weighted subspace fitting for general array error models," *IEEE Trans. Signal Process*., vol. 46, no. 9, pp. 2484-2498, Sep. 1998.
[33] S. Cao, Z. Ye, D. Xu, and X. Xu, "A hadamard product based method for DOA estimation and gain-phase error calibration," *IEEE Trans. Aerosp. Electron. Syst*., vol. 49, no. 2, pp. 1224-1232, Apr. 2013.
[34] P. Chen, Z. Cao, Z. Chen and X. Wang, "Off-grid DOA estimation using sparse bayesian learning in MIMO radar with unknown mutual coupling," *IEEE Trans. Signal Process*., vol. 67, no. 1, pp. 208-220, Jan. 2019.
[35] F. Wen, J. Wang, J. Shi, and G. Gui, "Auxiliary vehicle positioning based on robust DOA estimation with unknown mutual coupling," *IEEE Internet of Things J*., vol. 7, no. 6, pp. 5521-5532, Jun. 2020.
[36] C. Yang, Z. Zheng, and W. Wang, "Calibrating nonuniform linear arrays with model errors using a source at unknown location," *IEEE Commun. Lett*., vol. 24, no. 12, pp. 2917-2921, 2020.
[37] W. Wang, R. Wu, J. Liang, and H. C. So, "Phase retrieval approach for DOA estimation with array errors," *IEEE Trans. Aerosp. Electron. Syst*. vol. 53, no. 5, pp. 2610-2620, Oct. 2017.
[38] H. Xu, Y. Tian, and S. Liu, "Linear-shrinkage-based DOA estimation for coherently distributed sources considering mutual coupling in massive MIMO systems," *Int. J. Electr. Commun*., vol. 126, pp. 1-6, 2020.
[39] G. Krieger and M. Younis, "Impact of oscillator noise in bistatic and multistatic SAR," *IEEE Geoscience Remote Sens. Lett*., vol. 3, no. 3, pp. 424-428, Jul. 2006.
[40] H. Kim, A. M. Haimovich, and Y. C. Eldar, "Non-coherent direction of arrival estimation from magnitude-only measurements," *IEEE Signal Process. Lett*., vol. 22, no. 7, pp. 925-929, Jul. 2015.
[41] H. G. Park, C. Park, H. Oh, and M. G. Kyeong, "RF gain/phase and I/Q imbanlance error correction technique for multi-channel array antenna systems," in *Proc. IEEE VTS 53rd Veh. Technol*., Rhodes, Greece, May 2001, pp. 175-179.
[42] M. Eineder, "Ocillator clock drift compensation in bistatic interferometric SAR," in *Proc. 2003 IEEE Int. Geos. Remote Sensing Sym. (IGARSS)*, Toulouse, France, Jul. 2003, pp. 1449-1451. 1449C1451.
[43] W. Zhang, W. Liu, S. L. Wu, and J. Wang, "Robust DOA estimation for a MIMO array using two calibrated transmit sensors," in *Proc. the IET International Radar Conference*, Xian, China, April 2013.
[44] S. Haykin and K. J. L. Ray, *Handbook on Array Processing and Sensor Networks*. Hoboken, NJ: Wiley, 2010.
[45] Y. Tian, J. Shi, H. Yue, and X. Rong, "Calibrating nested sensor arrays for DOA estimation utilizing continuous multiplication operator," *Signal Process*., vol. 176, pp. 1-11, 2020.
[46] B. Liao and S. C. Chan, "Direction finding with partly calibrated uniform linear array," *IEEE Trans. Antennas Propaga*., vol. 60, no. 2, pp. 922-929, Feb. 2012.
[47] L. Huang and H. C. So, "Source enumeration via MDL criterion based on linear shrinkage estimation of noise subspace covariance matrix," *IEEE Trans. Signal Process*., vol. 61, no. 19, pp. 4806-4821, Oct. 2013.
[48] M. Trigka, C. Mavrokefalidis, and K. Berberidis, "An effective preprocessing scheme for DoA estimation in hybrid antenna arrays," in *Proc. 2018 25th Int. Conf. Telecommunications (ICT)*, Saint-Malo, France, Jun. 2018, pp. 127-131.
[49] S. Li, Y. Liu, L. You, *et al*., "Covariance matrix reconstruction for DOA estimation in hybrid massive MIMO systems," *IEEE Wireless Commun. Lett*., vol. 9, no. 8, pp. 1196-1200, Aug. 2020.
[50] P. Vallet, P. Loubaton, "Toeplitz rectification and DOA estimation with music," in *Proc. ICASSP*, Firenze, Italy, May 2014, pp. 2237-2241.
[51] K. Han, P. Yang, and A. Nehorai, "Calibrating nested sensor arrays with model errors," *IEEE Trans. Antennas Propaga*., vol. 63, no. 11, pp. 4739-4748, Sep. 2015.

Ye Tian (S'13-M'19) received the B.S. and Ph.D. degrees from the College of Communication Engineering, Jilin University, Changchun, China, in 2009 and 2014, respectively. He won a Huawei scholarship in 2013 and was selected as a young top talent by the Hebei Provincial Department of Education in 2016. He is currently an Associate Professor in Faculty of Information Science and Engineering, Ningbo University. He has published more than 30 international peer-reviewed journal/conference papers and more than 10 patents. His research interests include array signal processing, autonomous vehicle positioning, massive MIMO as well as large-dimensional random matrix theory.

Wei Liu (S'01-M'04-SM'10) received his BSc and LLB. degrees from Peking University, China, in 1996 and 1997, respectively, MPhil from the University of Hong Kong in 2001, and PhD from the School of Electronics and Computer Science, University of Southampton, UK, in 2003. He then worked as a postdoc first at Southampton and later at the Department of Electrical and Electronic Engineering, Imperial College London. Since September 2005, he has been with the Department of Electronic and Electrical Engineering, University of Sheffield, UK, first as a Lecturer and then a Senior Lecturer. He has published about 350 journal and conference papers, five book chapters, and two research monographs titled "Wideband Beamforming: Concepts and Techniques" (John Wiley, March 2010) and "Low-Cost Smart Antennas" (by Wiley-IEEE, March 2019), respectively. His research interests cover a wide range of topics in signal processing, with a focus on sensor array signal processing and its various applications, such as robotics and autonomous systems, human computer interface, radar, sonar, satellite navigation, and wireless communications.

He is a member of the Digital Signal Processing Technical Committee of the IEEE Circuits and Systems Society (Secretary from May 2020) and the Sensor Array and Multichannel Signal Processing Technical Committee of the IEEE Signal Processing Society (Chair from Jan 2021). He was an Associate Editor for IEEE Trans. on Signal Processing (2015-2019) and IEEE Access (2016-2021), and is currently an editorial board member of the journal Frontiers of Information Technology and Electronic Engineering and the Journal of The Franklin Institute.

He Xu received the B.Eng. and M.Eng. degrees from the College of Communication Engineering, Jilin University, Changchun, China, in 2010 and 2013, respectively. From September 2014 to December 2020, she worked as a Research Assistant in Yanshan University. She is currently pursuing the Ph.D. degree in Faculty of Information Science and Engineering, Ningbo University, Ningbo, China. Her main research interests are massive MIMO, integrated sensing and communication in 6G.

Shuai Liu (M'21) received the M.Eng. degree from the School of Resources and Information, China University of Petroleum, Beijing, China, in 2008, and Ph.D. degree from the Institute of Remote Sensing and Geographic Information System, Peking University, China, in 2012, respectively. He is currently a Lecturer with School of Information Science and Engineering, Yanshan University. His research interests include Intelligent remote sensing information processing, array signal Processing and machine learning.

Zhiyan Dong received the B.Eng. degree in Communication Engineering and Ph.D. degree in Mechanical and Aerospace Engineering from Jilin University, Changchun, China, in 2011 and 2016, respectively. He is currently an Associate Professor in Faculty of Institute of AI and Robotics, Fudan University. His research interests include wireless communications, intelligent control and perception, swarm for unmanned vehicle.